Geological Carbon Dioxide Storage
Technology Research Association

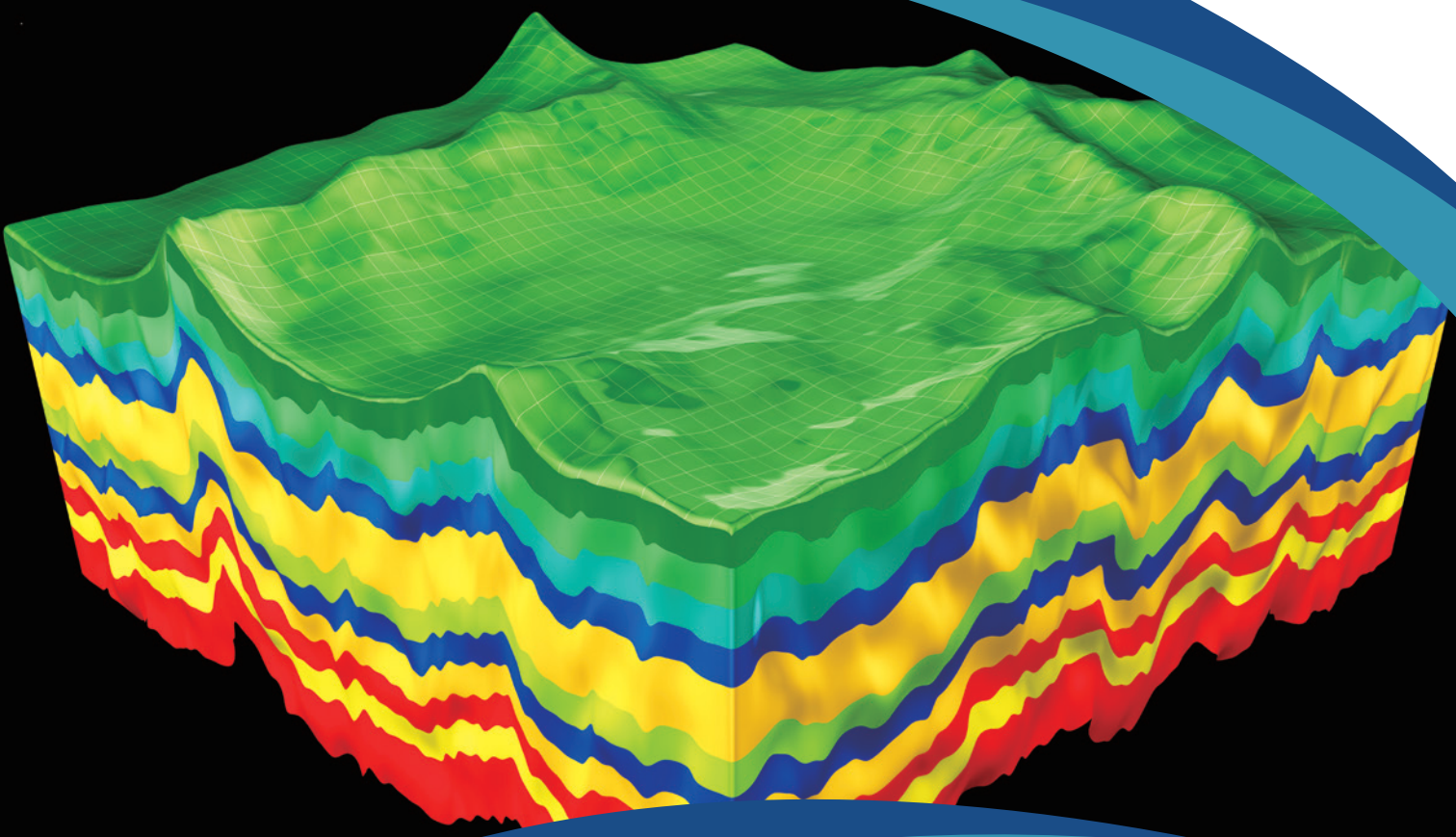

Practical Guidance for
Geological CO_2 Storage

Phase 03

Site characterization

S1 Nagaoka CO_2 pilot-scale injection test project

S1.1 Outline

RITE entrusted with operations commissioned by the Ministry of Economy, Trade and Industry has conducted CO_2 pilot-scale injection tests in addition to basic research, including basic experiments, studies of monitoring techniques, simulation technology development, and system research as "geological CO_2 storage technology development" since FY2000. The purpose of the CO_2 pilot-scale injection tests was to inject CO_2 into an actual aquifer, obtain data relating to its underground behavior, etc., verify safety and other related matters, and confirm the applicability of this technology.

In selecting a CO_2 pilot-scale injection test site in 2000, the Minami-Nagaoka Gas Field in Niigata Prefecture was selected from three candidate sites (Sarukawa Oil Field in Akita Prefecture, Minamiaga Oil Field in Niigata Prefecture, and Minami-Nagaoka Gas Field in Niigata Prefecture), and as injection sites, the Iwanohara base of (then) Teikoku Oil Co., Ltd., which owns the mining area of the gas field was assumed.

Evaluation of the candidate site as to its appropriateness as a CO_2 pilot-scale injection test site and whether pilot-scale tests were feasible (site characteristics evaluation) was conducted. Deliberation on the characteristics evaluation plan was conducted by the Promotion Committee, and obtainment of new geological data, including drilling of wells, and implementation of simulations, etc. were decided. For the site characteristics evaluation, three exploration wells were drilled from 2001 through 2002, and physical logging was conducted at each well. In addition, coring (spot coring) was conducted at two wells; where well data through analysis of the cores obtained there were comprehensively interpreted, and geological models were modified successively. In 2002, pumping tests, etc. were also conducted at the exploration wells, and simulations were conducted using various types of geotechnical information to show the feasibility of conducting CO_2 pilot-scale underground storage tests at the Iwanohara base, and a final decision on its implementation was made by the Research Promotion Committee. In 2003, the 3rd observation well was also drilled, and each of the previously drilled wells were diverted to an injection well and observation well.

After the implementation plans concerning injection and monitoring were formulated, injection started at an initial rate of 20 tons/day from July 2003, and then the injection rate was changed to 40 tons/day. The injection continued until January 2005 after a discontinuation period due to the occurrence of the Chuetsu Earthquake in October 2004, and the cumulative total injection was 10,405 tons.

Through implementation of diverse types of monitoring that was conducted during the Nagaoka pilot-scale tests, physical logging at the three observation wells, inter-well elastic wave tomography using the above data, repeated 3D elastic wave explorations, micro-vibration observations, and

other measures were conducted, by which a large amount of information was obtained. For understanding long-term behavior, monitoring continued over 15 years even after CO_2 injection was completed.

S1.2 Site characteristics evaluation

① Drilling of exploration wells

Although geological and various other data used in the process of site selection were publicly disclosed existing data, for site characteristics evaluation, new data were obtained. One of the reasons why the Iwanohara base was selected was the existence of prepared sites that were large enough to drill wells and build CO_2 injection and monitoring facilities.

The drilled exploration wells are shown in Figure S1.2-1, of which CO2-1 assuming a CO_2 injection well was drilled nearly vertically (the deviation was approximately 20m southward at a depth of the upper surface of the storage reservoir). The 2nd and 3rd wells were selected at drilling positions assuming future use as observation wells based on the initial simulations using geological data obtained by drilling the 1st well. CO2-2 (OB-2) was a directional well (97m eastward at the upper limit of the storage reservoir), and CO2-3 (OB-3) was a directional well (153m west-southwestward at the same limit). In addition, in 2003, at the project planning stage, an observation well CO2-4 (OB-4) was drilled at a position that was decided based on CO_2 migration predictions according to more detailed simulations. A directional well was drilled 78m west-northwestward at a depth of the upper limit of the storage reservoir, which was considered to be more efficient according to the monitoring plan.

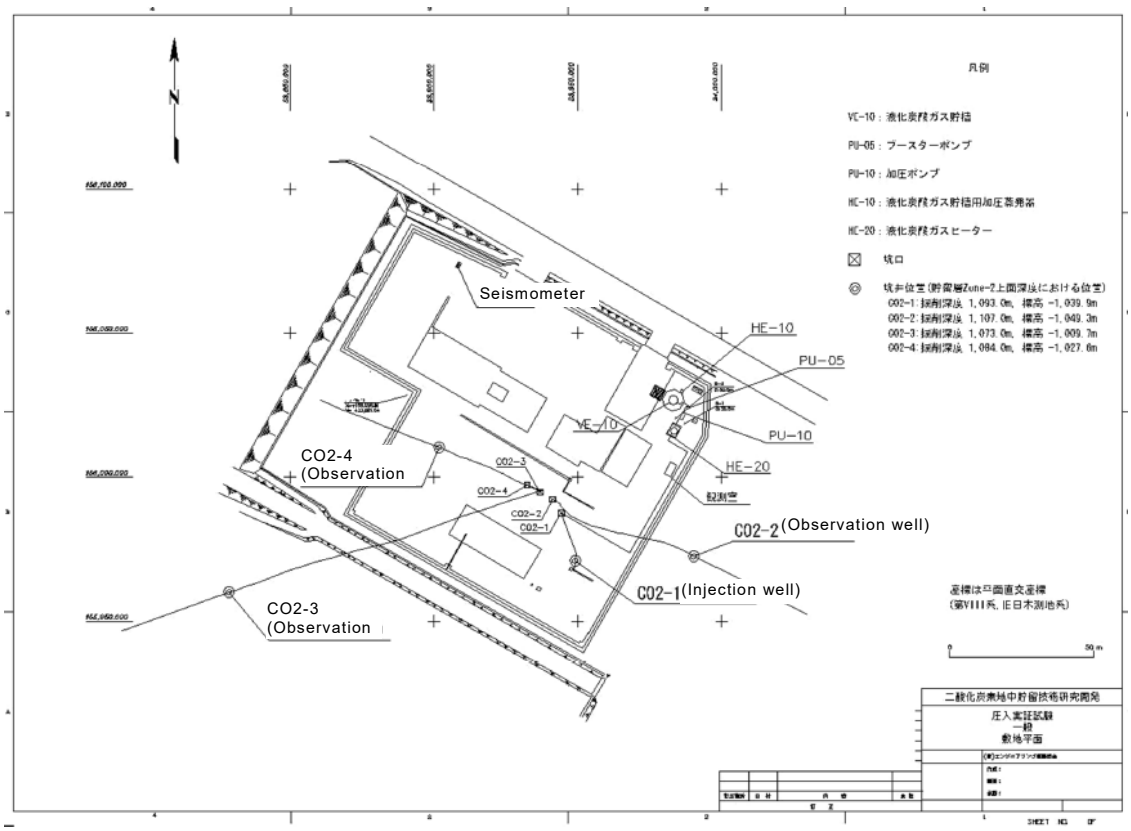

Figure S1.2-1 Well layout in the Nagaoka Demonstration Test Site (RITE, 2003)

② Obtainment of data at exploration wells

The following surveys and samplings were conducted during and after each well was drilled.

Cutting surveys and samplings: Cutting surveys (lithological surveys) were conducted at a depth of ≥300m for CO2-1, and at a depth of 900m or deeper (near the upper limit of the Haizume Formation) for other wells.

Mud gas measurements: Measurements were taken at a depth of around 300m or deeper.

Core samplings and observations: 45.0m and 17.5m cores were extracted from the storage reservoir at CO2-1 and CO2-2, respectively, and at the same time, geological observations and records were conducted.

Formation water sampling: When pumping tests were conducted, fluid samples (three) were taken from the storage reservoir.

Physical logging: At the three exploration wells, spontaneous-potential well-logging, gamma-ray logging, resistivity logging at a depth of approximately 300-350m or deeper, caliper logging, density logging, acoustic logging, neutron logging, resistivity logging by borehole imaging (FMI: Fullbore Formation Microimager), and nuclear magnetic resonance logging (CMR: Combinable Magnetic Resonance Tool) at a depth of around 900m or deeper were conducted. In addition, formation pressure and permeability logging (MDT: Modular Dynamic Tester) were conducted at 27 points of CO2-1 and CO2-2 (See

Figure S1.2-2 and Table S1.2-1.).

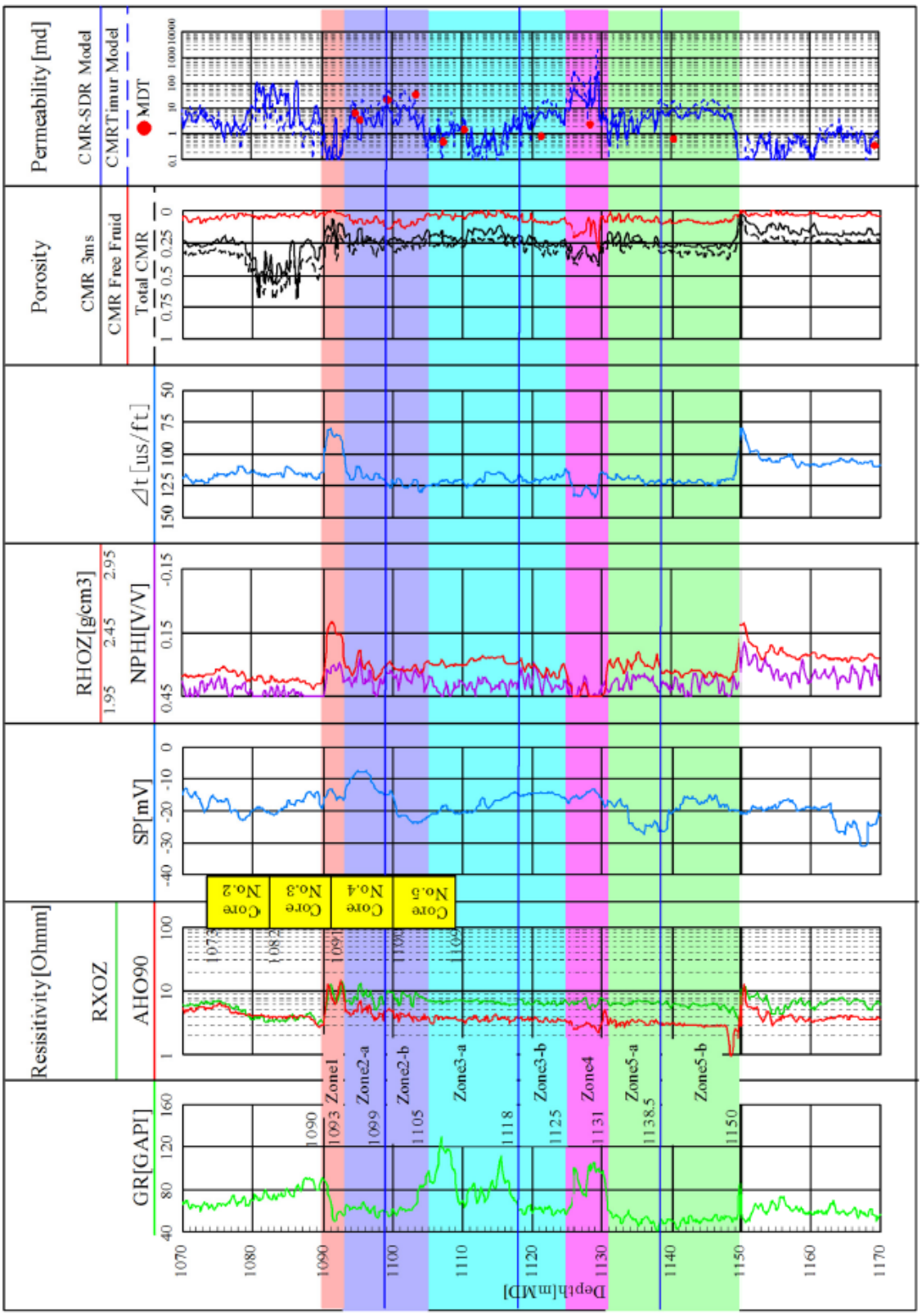

Figure S1.2-2 CO2-1 Well logs (RITE, 2002)

Table S1.2-1 Well logging results for each zone in "Ic" formation (RITE, 2003)

Zone	Thickness (m)	Lithofacies	Resistivity (Rt) Ωm	Density (ρb) g/cm^3	Sonic velocity (Δt) ms/ft	Gamma ray (GR) API	Nuclear magnetic resonance	Formation pressure, Permeability by MDT
1	3.0-4.8	Calcareous sandstone	2～15	2.10-2.60	80-115	60-90	Tight	Tight
2	9.0-12	very fine - fine Sandstone	4～7	2.00-2.35	100-130	55-120	Permeability, order of several tens of mD (millidarcies)	Permeability, order of several tens of mD
3	20.0-23.5	Granule, Sandstone	3～5	2.00-2.40	100-130	60-160	Permeability, poor – slightly well	
4	5.5-7.5	tuffaceous Sandstone, very fine Sandstone	3～4	1.80-2.25	120-130	50-110	Permeability, several hundreds of mD	Mobility, 2-4 md/cp
5	16.8-20.5	silty Sandstone	2～5	2.10-2.40	90-130	50-70		

③ Evaluations by core analysis

At the wells CO2-1 and CO2-2, spot cores were extracted and analyzed as shown in Table S1.2-2.

Table S1.2-2 Laboratory core test items (RITE, 2001)

Type of the analysis	Item of the analysis		Seal	Reservoir	Remarks
Cuttings analysis	X-ray fluorescence analysis		0	11	
Routine core analysis	Grain Density	circumferential	0	33	include 1 plug size core
		Longitudinal	0	9	
	Porosity	circumferential	0	33	include 1 plug size core
		Longitudinal	0	9	
	Air permeability	circumferential	0	33	Dry sample include 1 plug size core
		Longitudinal	0	9	Dry sample
Special core analysis	Relative permeability	Gas flood	0	5	
		Water flood	0	5	
	Capillary pressure measurement		0	5	Air/Water
	Ultrasonic velocity	Dry sample	0	2	
		Saturated sample	2	2	
	Displacement (threshold) pressure	Whole size	2	0	
		Plug size	2	0	

- General core tests

Targeting the Ic layer, general core tests of porosity and absolute permeability measurements were conducted. To prevent sampling location bias, 42 samples were taken from the entire area of the target cores. The data obtained here were used for injection planning and evaluations of the

storage reservoir capacity, etc.

By way of example, permeability measurement results are summarized in Table S1.2-3.

Table S1.2-3 Summary of permeability measurement from routine core analysis（RITE,2003）

Zone		Air permeability (md)				Water permeability (md)			
		Average	Minimum	Maximum	No. of data	Average	Minimum	Maximum	No. of data
Seal		-	-	-	0	-	-	-	0
Reservoir	Zone-1	27.7	-	-	1	-	-	-	0
	Zone-2	233.7	3.0	1,070.5	41	95.0	47.3	143.0	4
	Zone-3	39.9	7.4	87.6	11	4.4	-	-	1
	Zone-4	-	-	-	0	-	-	-	0
	Zone-5	-	-	-	0	-	-	-	0

- Special core tests

Targeting the storage reservoir of the Ic layer, 3 items of special core tests were conducted, including relative permeability (gas flood and water flood) and capillary pressure measurements. In each test, the number of samples was 5, which were taken from over entire target cores in order to prevent sampling location bias, wherever possible. The sampling data were used for input parameters in simulations, and other objectives.

Targeting the seal layer at the head of the Ic layer, displacement pressure (threshold pressure) measurements were also taken, which were used for evaluation of the sealing capacity. In addition, samples for P/S wave propagation velocity measurements targeted the Ic layer and the seal layer. The sampling data were used to examine the application of inter-well tomography.

④ Storage reservoir evaluation

From the results of physical logging and core analysis, each zone of the storage reservoir was evaluated as follows:

Zone-1: Hard, closely-packed, principally composed of calcareous sandstone. Regarded as an impervious zone from core observations, and also judged as poor in properties as a storage reservoir from the physical logging results.

Zone-2: Principally composed of fine to medium-grained sandstone, where a conglomerate layer is found to be intercalated and of granule content. The results of physical logging (formation pressure and permeability logging) including nuclear magnetic resonance logging showed the highest permeability. Similar evaluations were also made by core tests.

Zone-3: Composed of clumped ultrafine-grained sandstone, more pelitic compared to Zone-1 and 2, being high in the value of gamma-ray logging as 70 to 105 API. The results of physical logging (formation pressure and permeability logging) also show low permeability.

Zone-4: Pelitic, composed of tuffaceous sandstone and ultrafine-grained sandstone. As for the results of physical logging, nuclear magnetic resonance logging shows a slightly high permeability, but formation pressure and permeability logging show

low permeability.

Zone-5: Silty sandstone, indicates the existence of a mixture of sandy and pelitic parts. As for the results of gamma-ray logging, neutron logging, etc. are similar to Zone-2, but the results of physical logging (formation pressure and permeability logging) show low permeability.

⑤ Pumping tests

In order to understand the injection capacity of Zone-2 to 5, pumping tests were conducted at the injection well CO2-1. The purpose of the tests were the following three points, and the inside of the pit is shown in Figure S1.2-3 and Figure S1.2-4.

- To calculate the production index (PI) of the layer subject to CO_2 injection and estimate the CO_2 injection capacity
- To conduct pressure analysis and calculate the permeability and skin around the well from the results of the analysis
- To sample produced water and obtain information on formation water

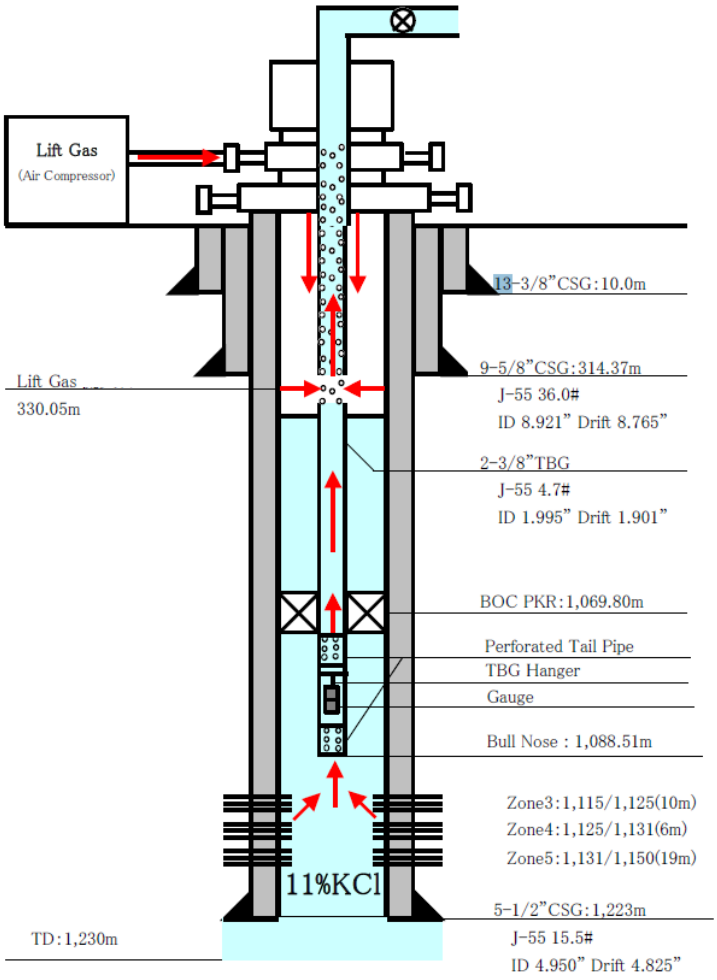

Figure S1.2-3 Well configuration (@Production test Zone-3 to 5 (No.1)) (RITE, 2003)

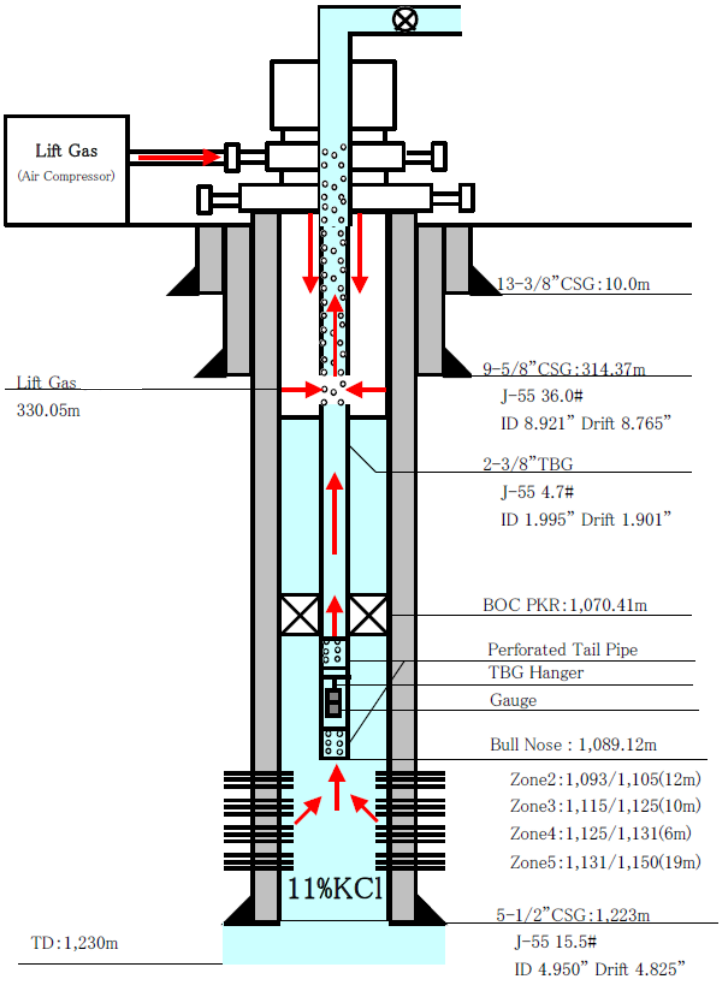

Figure S1.2-4 Well configuration (@Production test Zone-2 to 5 (No.2)) (RITE, 2003)

- Results of pumping tests

Test No. 1 was conducted on Zone-3, 4, and 5 that were considered to have relatively low permeability. Pumping test No. 2 was conducted by adding a section of Zone-2 that was considered to have high permeability. The purpose of the tests were achieved as follows:

- Test No. 1 was conducted on sections of Zone-3, 4, and 5, where it was expected that permeability was relatively low, but flowing was possible at a stable rate of 5.6KL/d. Test No. 2 was conducted by adding the section of Zone-2 to the target, where flowing was possible at a stable rate of 21.4KL/d.
- At the completion of test No. 2, formation water was sampled.
- Based on the records of bottom hole pressure measurements, the production index (PI) was obtained. Results obtained showed that the PI of the Zone-3, 4, and 5 sections was 0.17KL/d/ksc from test No. 1, and the PI of the total including Zone-2 was 0.70KL/d/ksc from test No. 2.
- Pressure analysis was conducted by using the records of enclosed bottom hole pressure

measurements. Results obtained showed that the permeability of Zone-3, 4, and 5 was approximately 0.52mD from test No.1, and the permeability of Zone-2, 3, 4, and 5 was approximately 2.1mD from test No.2. The permeability of Zone-2 calculated from the above is 6.43mD.

As a result of the above well tests, it was decided that the injection layer was Zone-2. Although the permeability was a value lower than expected and the PI was worse than expected, it was highly likely that 40 tons/day could be injected even with the assumed compressor, and it was considered that 40 tons/day could be injected by simply decreasing the skin through the implementation of acid treatment, etc. even in the case where the krg value was small and 40 tons/day could not be injected during a steady-state period. The results are shown in Table S1.2-4.

The results of the above pumping tests provided important information for the development of geological models as well as simulations.

Table S1.2-4 Results of production tests in 2002 (RITE, 2003)

		No.1 Production (Drawdown) test		No.2 Production (Drawdown) test	
P_i	[psia]	1591			
r_w	[ft]	0.354			
C_t	[l/psi]	7.00E-06			
μ	[cp]	0.61			
Bt	[rb/stb]	1.00			
φ	[fraction]	0.22			
h	[ft]	114.8		154.2	
q	[stb/d]	35.22		134.59	
T_P	[hours]	47.20		45.04	
pwf	[psia]	1120.72		1162.38	
		PDD*1	PBU*2	PDD*1	PBU*2
C	[stb/psi]	4.65E-05	0.0477	4.65E-05	0.0480
skin	[-]	6.88		6.88	
Reservoir Model		Homogeneous & infinite Acting			
k	[md]	0.68		2.33	
r_{inv}	[ft]	125		314	
PI	[stb/d/psi]	0.075		0.314	
	[kl/d/ksc]	0.169		0.710	
ΔP_s	[psi]	267.36		221.99	
PI_{ideal}	[stb/d/psi]	0.174		0.651	
	[kl/d/ksc]	0.392		1.473	

*1 PDD : Pressure Draw-Down

*2 PBU : Pressure Build-Up

⑥ Seal layer evaluation

The seal layer is pelitic directly above Zone-1 of the Ic layer of the Haizume Formation. The apparent layer thickness is 131.5 - 149.5m, which is about double the storage reservoir (apparent layer thickness: 56.6 - 66.0m). The lithofacies are mainly mudstone, intercalated with ultrafine to fine-grained sandstone. The mudstone is gray to dark-gray, and is partially olive-colored. In addition, in the range of surveys conducted by drilling new exploration wells (a range with a radius of approximately 120m, centering on CO2-1), inter-well lithostratigraphy and lithofacies contrast were good, and the continuity of the seal layer was judged to be good.

Although the results of formation pressure and permeability logging of this horizon were obtained in only one place (the well CO2-1, 1,055.2m in depth), the converted permeability is as small as 0.14mD. In addition, the threshold pressure value obtained by core tests exceeds 1.38MPa, which is 176m or more in terms of gas column conversion (Table S1.2-5).

Table S1.2-5 Displacement (threshold) pressures in seal at the well CO2-1 (RITE, 2002)

Well	Sample No.	Depth (m)	Zone	Lithofacies	Type of sample	Threshold pressure (MPa)	Gas column (m)
CO2-1	C-1	985.09-985.32	Seal	Mudstone	Plug	>1.38	176
CO2-1	B -1	1,087.03-1087.30	Seal	Mudstone	Full diameter core	>5.52	706
CO2-1	B -2	1,087.71-1087.89	Seal	Mudstone	Plug	>2.76	353
CO2-1	A	1,090.69-1,090.95	Zone-1	Mudstone	Full diameter core	>13.79	1,764

Gas density of 0.5 g/cm^3 was used in gas column calculations. Plug = 1"1/2 diameter, 5-7 cm long; full diameter core = 3"6/8 diameter, approx. 20 cm long)

From the above data, it is judged that this seal layer has sufficient CO_2 sealability in the storage reservoir. In addition, development of many mudstone layers between the seal layer and ground surface is known from existing wells and newly drilled wells.

It is considered to be unlikely that faults and other discontinuity planes exist between the seal layer and ground surface, which could become types of leakage routes, from the following points.

Geological layers between the exploration wells in the storage site and between those wells and existing wells outside the site can be easily contrasted in correspondence with their structures (stratal dips), and there is no need to expect faults between them.

In the existing elastic wave exploration results, no faults are found reaching the storage reservoir from the vicinity of the ground surface.

No discontinuity plane with the potential for contrast to the Oyazawa Fault extends to the depth of the storage reservoir.

As mentioned above, with the properties shown by the core analysis results as a seal layer, it is evaluated that the pelitic section of the Haizume Formation sufficiently functions as a seal layer according to the logging of the pelitic section of the Haizume Formation developing at the head of the Ic layer (injection layer) of the Haizume Formation, as well as the thickness of the pelitic section, its horizontal extent, and the presence or absence of faults cutting it.

⑦ Geological model updating and simulations and studies to predict CO_2 injection behavior

- New data

In FY2000, as part of the Nagaoka site characteristics evaluation pertaining to the pilot-scale injection tests, storage reservoir model updating was conducted by reflecting the core data of the exploration well CO2-1, and CO_2 distribution in the pilot-scale injection tests was predicted.

In FY2001, geological models were modified and simulations were conducted by analyzing the results of logging at the exploration well CO2-1, and obtaining core analysis results, and the results of logging at the wells CO2-2 and CO2-3, which were the data of formation pressure and permeability logging and nuclear magnetic resonance logging in particular.

- Review of parameters

Effective permeability

In the special core analysis, relative permeability was measured by applying circumferential pressure with 5 core plugs, and in the process, permeability under 100% water saturation was observed. This permeability corresponds to effective permeability in underground conditions reflecting the effects of formation stress and irreducible water saturation. Figure S1.2-5 shows plots of air permeability measured with the same core plugs as the water permeability obtained in this special core analysis, and it is clear that they correlate very well. Coincidence with the permeability by magnetic resonance logging is also good. From the above, it was judged that a fairly realistic effective permeability of the storage reservoir was obtained from the core analysis results.

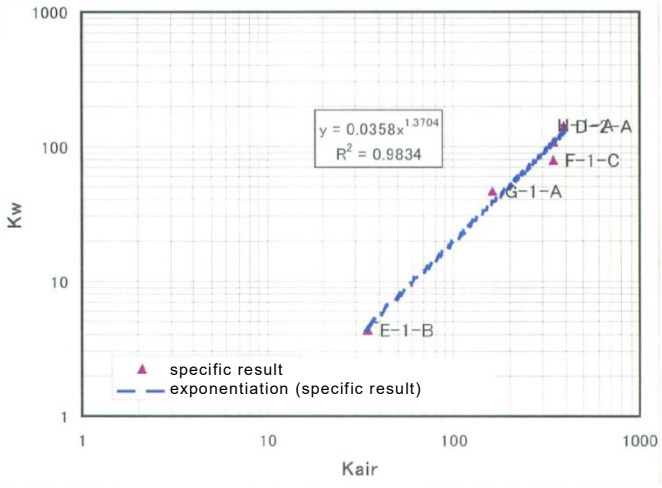

Figure S1.2-5 Correlation between effective water permeability and air permeability (RITE, 2002)

As shown in Figure S1.2-6, the air permeability of Zone-2 in general core analysis shows an approximately lognormal distribution, and it is considered that the effective permeability converted by using the above correlation shows a similar distribution. The distribution is irregular because of an insufficient number of data points. Therefore, as the effective permeability of the entire Zone-2, not a simple arithmetic mean but a median was adopted, which was 23.0mD. In addition, the permeabilities of other zones than Zone-2 were as follows: Zone-1=0mD, Zone-3=0.88mD, Zone-4=1.42mD, and Zone-5=0.35mD.

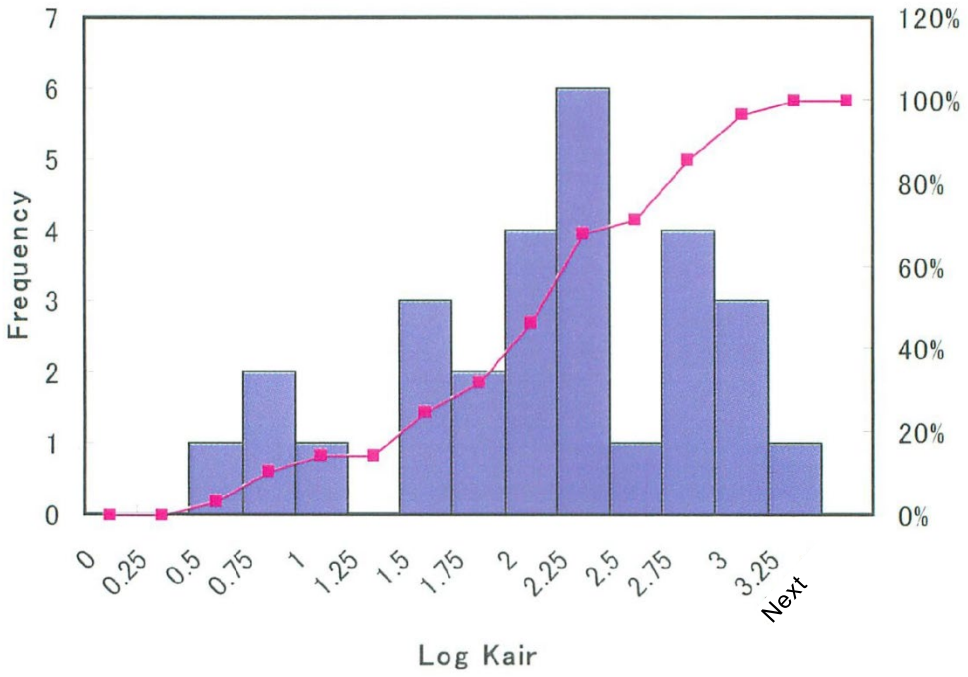

Figure S1.2-6 Frequency distribution of air permeability from core analysis (RITE, 2002)

Irreducible Water Saturation, S_{wir}

As seen in Figure S1.2-7, for the 5 core plugs used for the special core analysis, a strong correlation was obtained between the irreducible water saturation and $\sqrt{(k_w/\varphi)}$. When Zone-2's representative values φ=31.5% and kw=23mD are applied to the approximate expression for correlation, the irreducible water saturation of this zone becomes 81.8%.

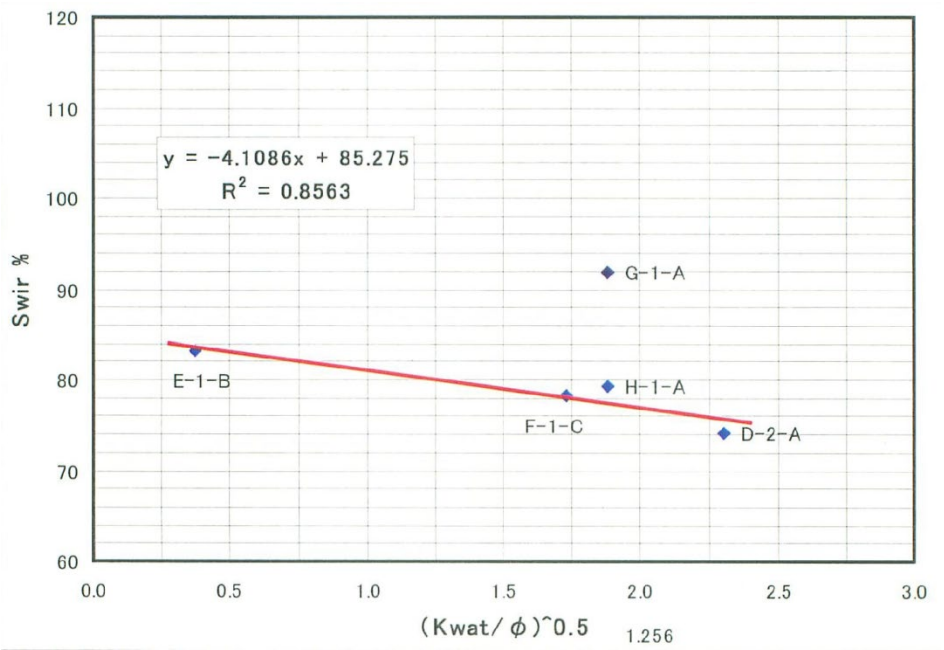

Figure S1.2-7 Correlation between irreducible water saturation and $\sqrt{(kw/\phi)}$ (RITE, 2002)

Residual Gas Saturation, S_{gr}

A strong correlation was shown between the residual gas saturation and initial gas saturation. From this correlation, 13.1% was taken for the residual gas saturation of Zone-2. With all 5 core plugs used for the special core analysis, showing that the critical gas saturation, S_{gc} was extremely small, it was judged that there was no problem with S_{gc}=0%.

Effective gas permeability at irreducible water saturation, $k_g@S_{wir}$

With respect to the core data, for kw=23mD of Zone-2, set were $k_g@S_{wir}$ plane=1.65, and $k_{gr}@S_{wir}$=0.0717.

Relative Permeabilities

When measured relative permeabilities are normalized with respect to endpoints, curves seen in Figure S1.2-8 are obtained. As there are considerable variations, it is not entirely appropriate to average these curves as they are. Therefore, the 4 curves excluding the G-1-A data were averaged, which was taken as a representative curve of Zone-2. What was obtained by using the endpoint

values of Zone-2 described above were the gas-water relative permeabilities shown in Figure S1.2-9.

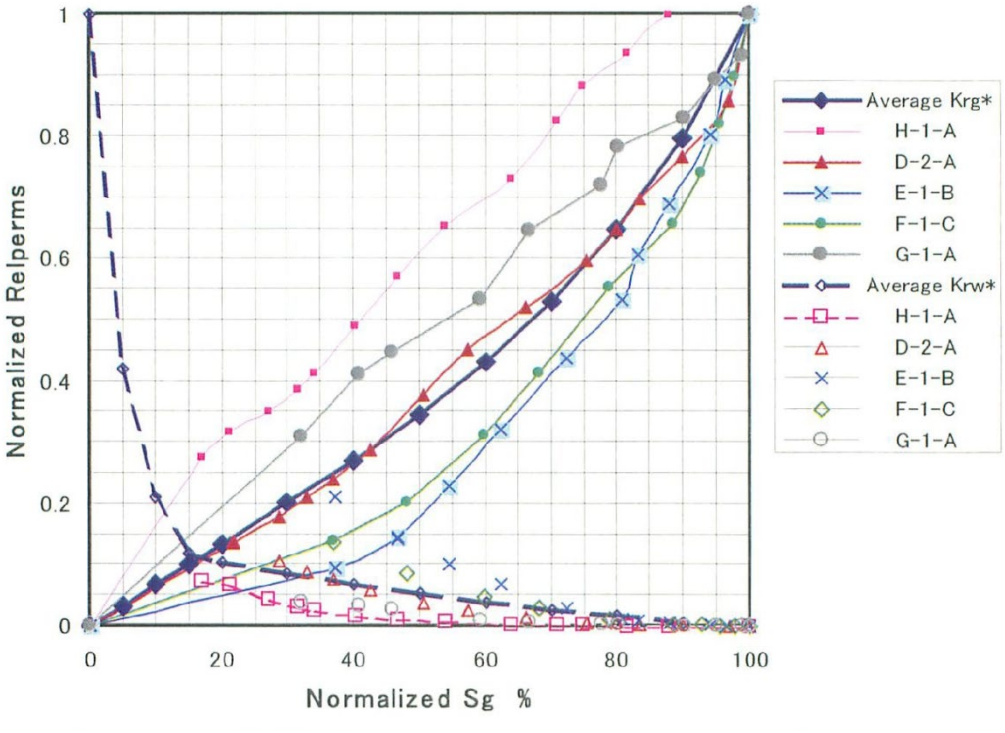

Figure S1.2-8 Averaged normalized relative permeability curves (RITE, 2002)

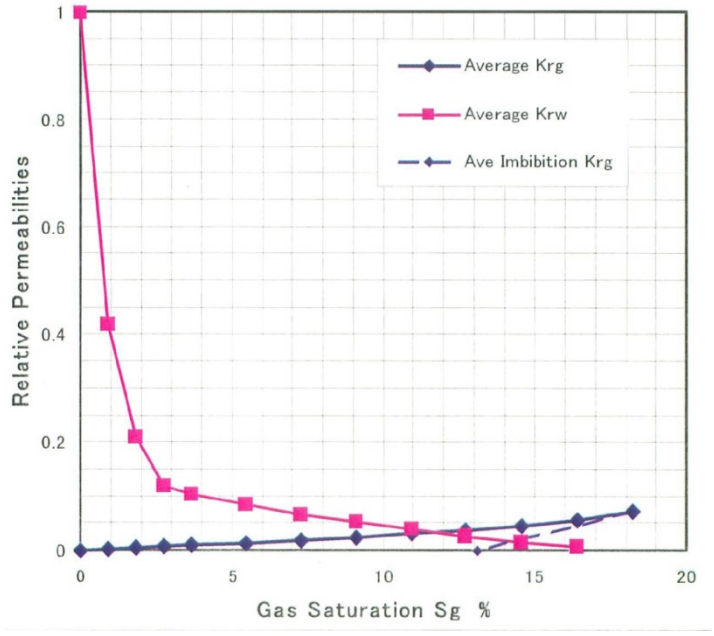

Figure S1.2-9 Gas-water relative permeability for Zone-2 (RITE, 2002)

Other parameters (Table S1.2-6)

Table S1.2-6 Key parameters of the reservoir model (RITE, 2002)

Formation Pressure	114.3	kgf/cm^2 @ 1,049.2 mSS
Formation Temperature	50	C
Gross Thickness	10-60	m
Net/Gross Ratio	1.0	
Porosity (=constant)	20-25	%
Horizontal Permeability (k_x=k_y=constant)	1-23	md
Vertical-Horizontal Permeability Ratio	0.25	
Pore Compressibility	$4*10^{-6}$	psi^{-1}
Irreducible Water Saturation	81.8	%
Critical Gas Saturation	0	%
Residual Gas Saturation	13.1	%
Gas Relative Permeability @ S_{wir}	0.0717	
Relative Permeability	Curves from Core Analysis	
CO_2 Gas Phase Density	0.477	g/cc @ Reference Reservoir Condition
CO_2 Solubility in Water	27	Nm^3/Nm^3 of water
CO_2 Injection Rate	40	tons/day (21,500 Nm^3/day)
Cumulative CO_2 Injected	20,000	tons (10,750,000 Nm^3)
Perforation Interval	Zone 2-5	(56 m)
Simulation Grid	89*142*5	(No. of Grid Blocks=63,190)
Areal Dimensions of a Grid Block	25m*25m	in the area of CO_2 distribution
	50m*50m	in the injection well - structure top area
	200m*200m	outside the refined area
Vertical Dimension of a Grid Block	4-22 m	according to the layering of the Ic formation

- FY2001 simulations and studies, and their results

Out of the calculation results, the distribution of gas-phase saturation in Zone-2 at the time of 20,000 tons injection is shown in Figure S1.2-10, and the distribution of gas-phase saturation at the WNW-ESE cross-section passing through the injection well is shown in Figure S1.2-11. In addition, the distribution of the amount of dissolved gas per unit volume of the storage reservoir in Zone-2 at the time of 20,000 tons injection is shown in Figure S1.2-12, and the amount of dissolved gas at the WNW-ESE cross-section is shown in Figure S1.2-13.

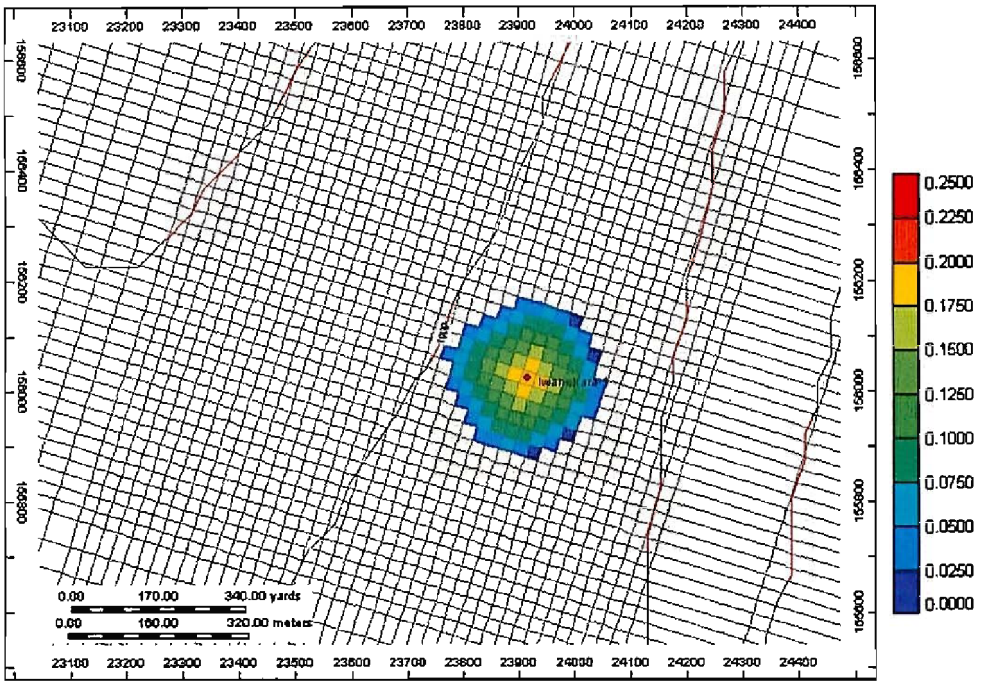

Figure S1.2-10 Distribution of gas phase saturation (fraction) in Zone-2 at 20,000 tons injection based on year 2001 model (RITE, 2002)

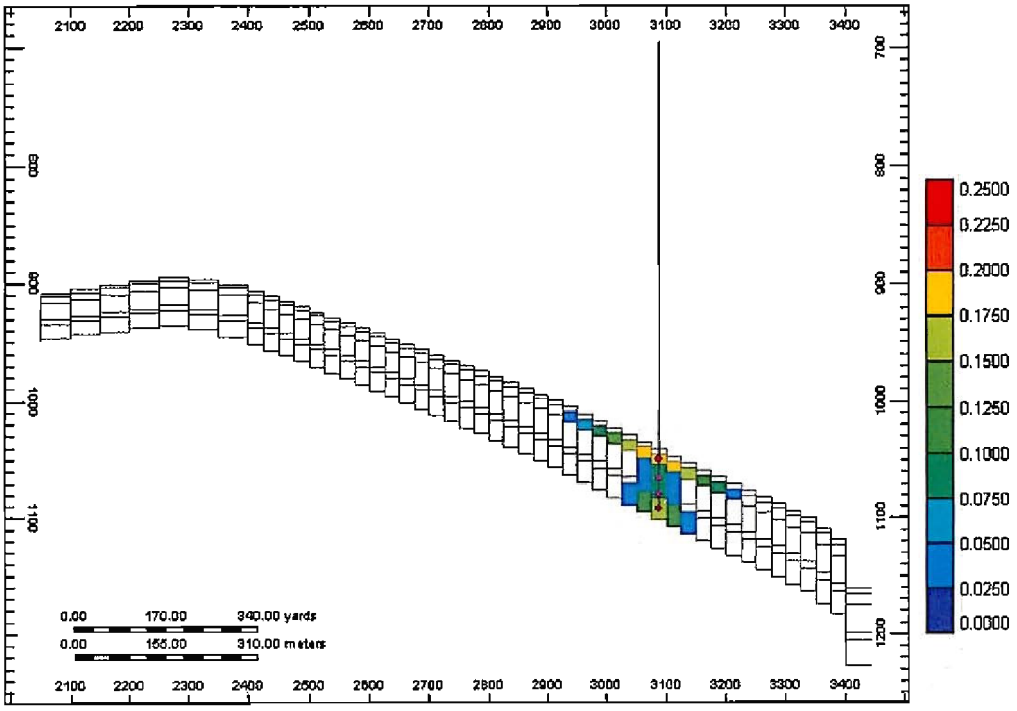

Figure S1.2-11 Distribution of gas phase saturation (fraction) in Zone-2 at 20,000 tons injection based on year 2001 model (RITE, 2002)

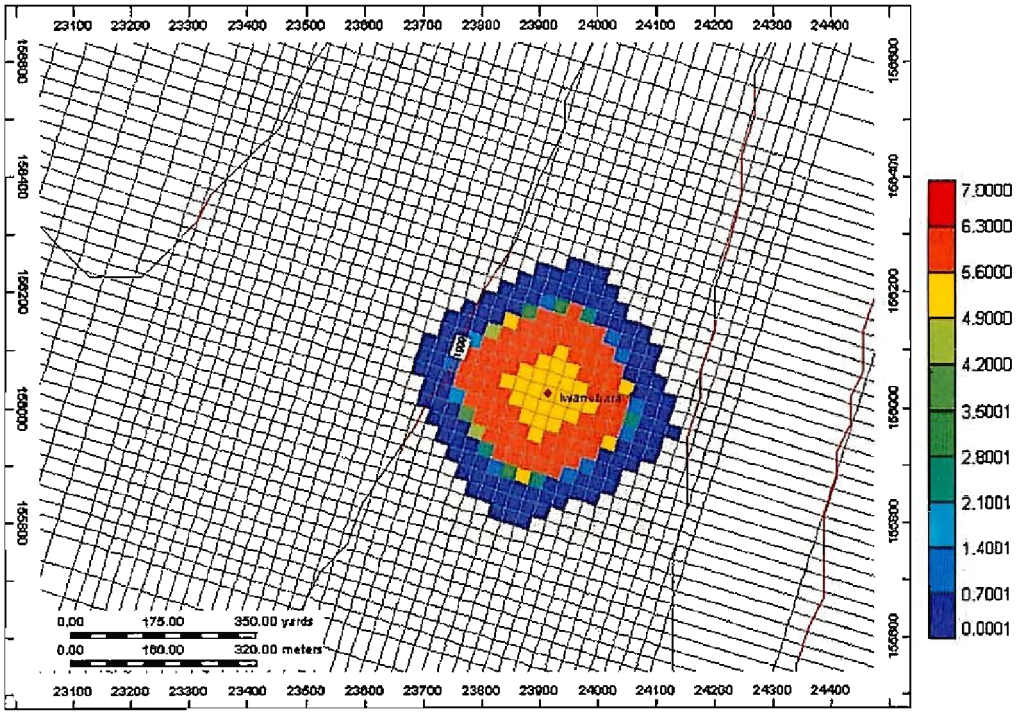

Figure S1.2-12 Distribution of dissolved gas per unit reservoir volume (sm^3CO_2/m^3 reservoir) in Zone-2 at 20,000 tons injection using year 2001 model (RITE, 2002)

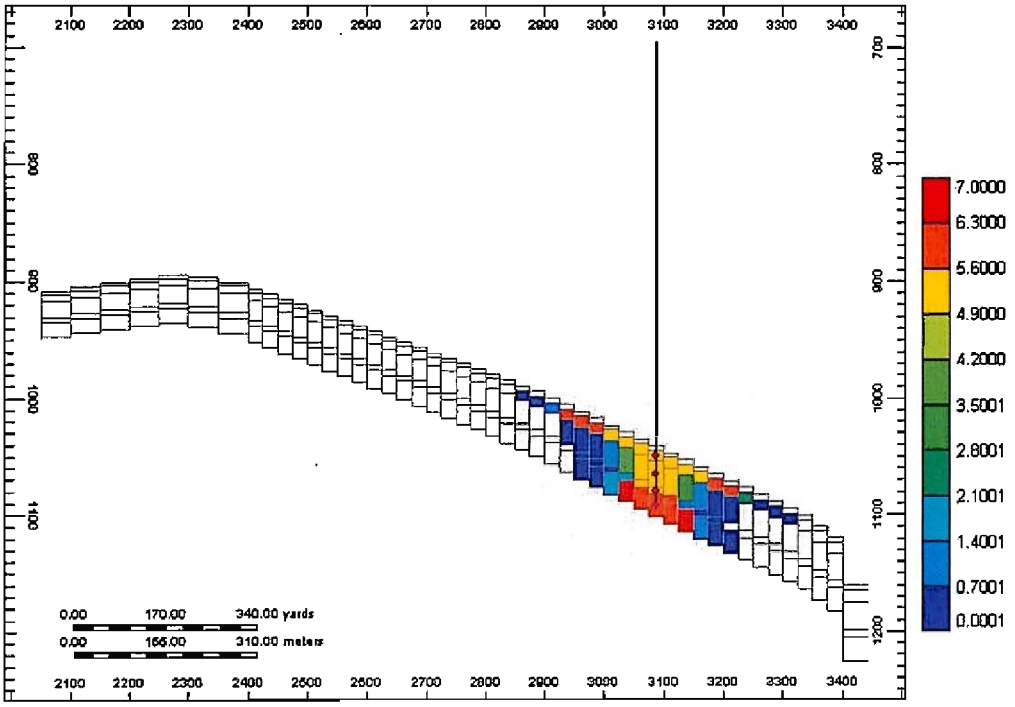

Figure S1.2-13 Distribution of dissolved gas per unit reservoir volume (sm^3CO_2/m^3 reservoir) in the WNW/ESE cross section at 20,000 tons injection using year 2001 model (RITE, 2002)

Figure S1.2-14 shows the pressure distribution (pressure increase from the initial pressure) in Zone-2 at the time of completion of 20,000 tons injection. It is expected that the pressure rise is

23kgf/cm^2 in the immediate vicinity of the injection well, and is about 6.5kgf/cm^2 at a 200m radius. Figure S1.2-15 shows distributions of changes (kgf/cm^2) from the initial pressure at the WNW-ESE cross-section at the time of completion of 20,000 tons injection. As can be seen in Figure S1.2-16, the injection bottom hole pressure increases slightly until a certain level of gas-phase saturation is reached in proximity to the injection well, but it becomes nearly constant 100 days after the start of injection, which is about 44kgf/cm^2 higher than the initial formation pressure. It was predicted that the wellhead injection pressure required was 158kgf/cm^2 at maximum, and was around 80kgf/cm^2 after the pressure was brought into a steady state.

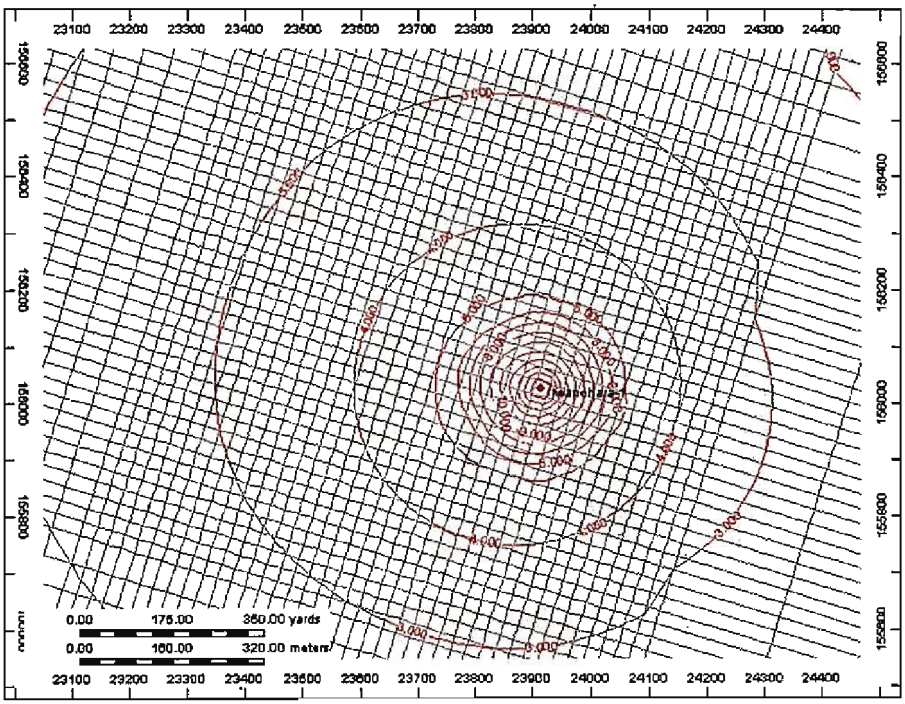

Figure S1.2-14 Change from the initial pressure (kg/cm^2) in Zone-2 at the completion of the 20,000 tons injection by the year 2001 model (RITE, 2002)

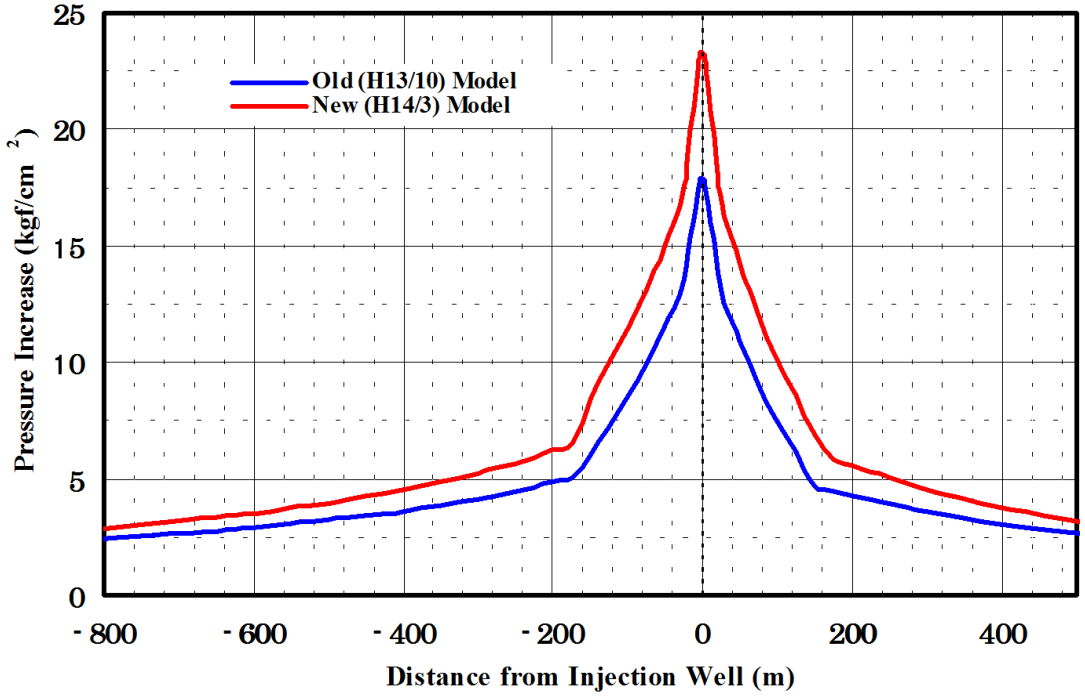

Figure S1.2-15 Change from the initial pressure in WNW-ESE cross section at completion of 20,000 tons injected (kgf/cm^2 distribution, red is 2001 final version (RITE, 2002))

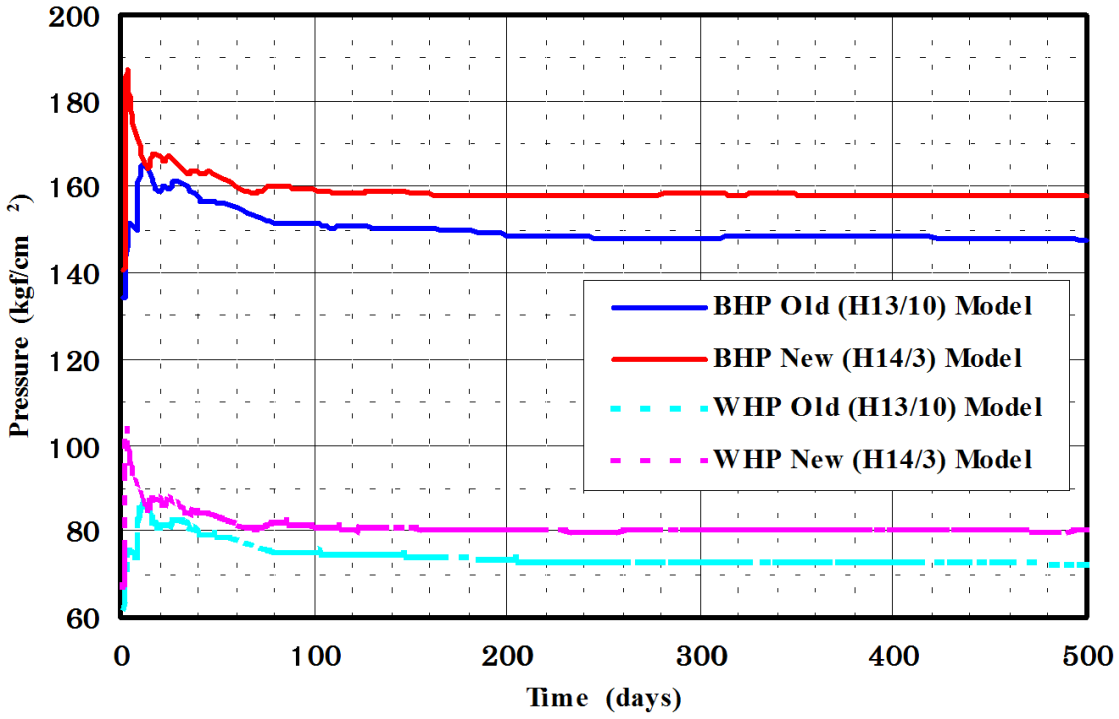

Figure S1.2-16 Injection bottom hole pressure and wellhead pressure changes over time, red is the final version for year 2001 (RITE, 2002)

References

1) RITE (2001): Reports on Geological Carbon Dioxide Research
2) RITE (2002): Reports on Geological Carbon Dioxide Research
3) RITE (2003): Reports on Geological Carbon Dioxide Research
4) RITE (2004): Reports on Geological Carbon Dioxide Research

S2 Characteristics evaluation of the Tomakomai large-scale demonstration test site

S2.1 Purpose

Based on the "For Safe Operation of a CCS Demonstration Project" (guideline) by the Ministry of Economy, Trade and Industry, site characteristics were evaluated, including the matters to be complied with from the aspects of safety and environment of large-scale demonstration tests in addition to the appropriateness of the storage reservoir and seal layer of the Tomakomai demonstration test site. The following is an introduction to the outline of the characteristics evaluation of the Tomakomai large-scale demonstration test site based on the evaluation report by the expert panel of the Ministry of Economy, Trade and Industry.

S2.2 Outline of regional geological surveys

As a result of the nation's basic geophysical explorations and petroleum and natural gas development activities by private companies, there is a significant amount of regional subsurface information. Figure S2.2-1 shows the outline of regional geology around Tomakomai. In this survey area, fold structures have been found in parallel at intervals of about 10km in the north-south direction or in the north-northwest-south-southeast direction. In addition, the anticlinal structures on the east side have undergone deformations accompanied by reverse faults, while it is interpreted that all the anticlinal structures on the west side, including the survey area, are of relatively weak deformations.

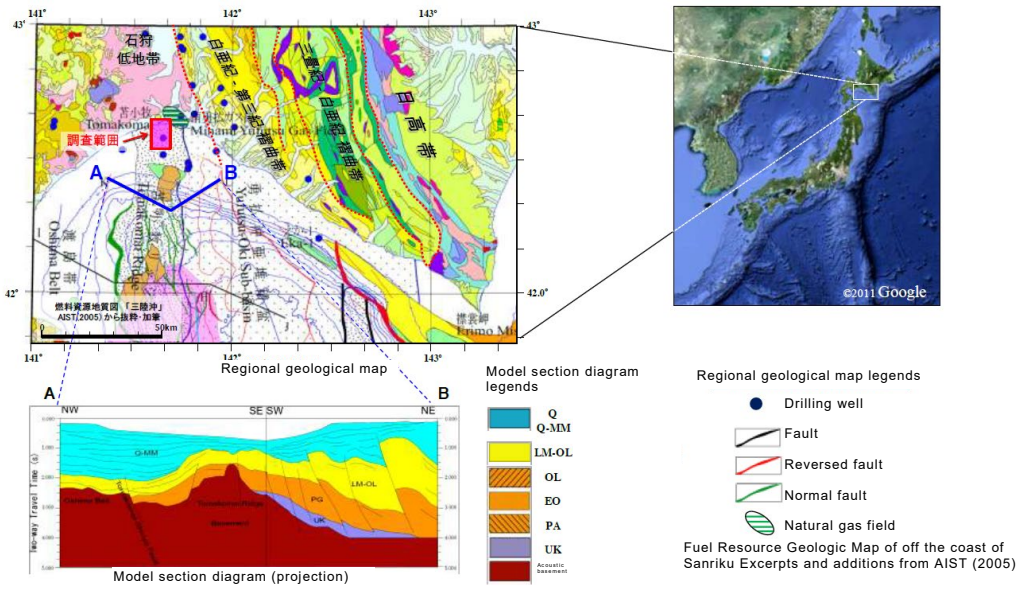

Figure S2.2-1 Regional geological map and schematic cross section around Tomakomai(METI,2011)

S2.3 Outline of new geological surveys

In the nearshore waters of the West Port zone of the Tomakomai Port, elastic wave exploration surveys and deep subterranean (depth: 3,000m) well drilling for petroleum and natural gas development have already been conducted; therefore, as layers intended for CO_2 storage, the Moebetsu Formation and the T1 Member of the Takinoue Formation distributed approximately 1,000m to approximately 3,000m under the seabed have been known. In order to conduct large-scale demonstration tests, the following geological surveys were newly

conducted during FY2009 - FY2011.

1) Three-dimensional elastic wave exploration

At the offing of the West Port zone of the Tomakomai Port, three-dimensional elastic wave exploration data were acquired in the range of approximately 3.8km east-west and approximately 4.1km north-south in FY2009, and in the range of approximately 5.9km east-west and approximately 7.6km north-south in FY2010 (Figure S2.3-1). This additional survey range includes private Well A.

2) Exploration well drilling

In FY2010, Tomakomai CCS-1 was drilled, where physical logging, leak-off tests (strength measurements of the seal layer), core sampling and cuttings sampling, injection tests of the storage reservoir, etc. were conducted. In the analysis of physical properties of the core samples and cuttings samples, porosity, permeability, and threshold pressure were measured. In FY2011, Tomakomai CCS-2 was drilled, where similar analytical tests on physical properties were conducted.

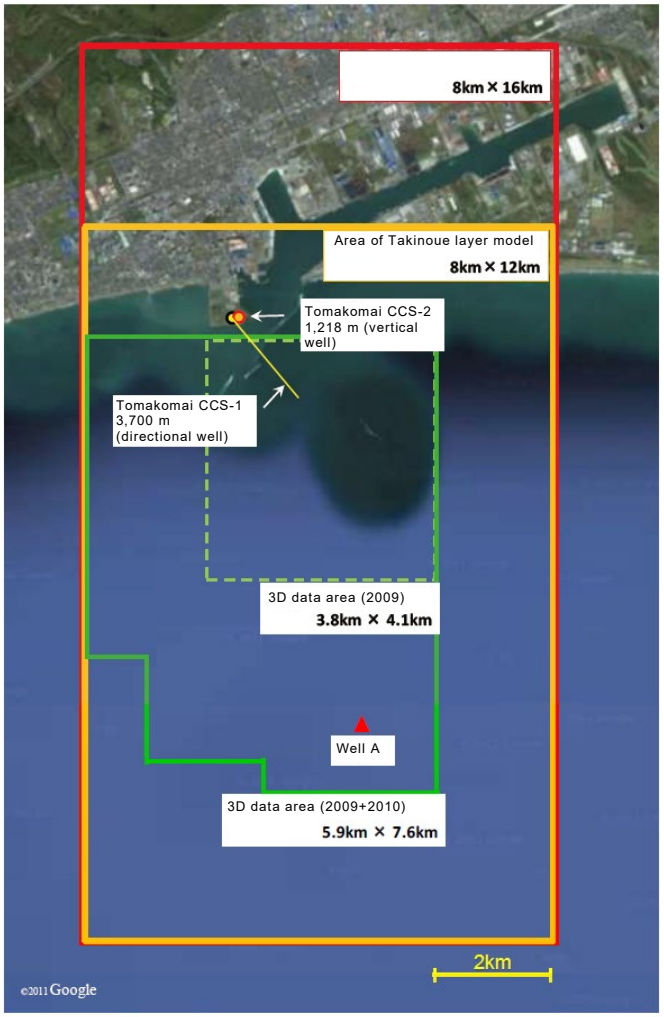

Figure S2.3-1 Survey area (METI,2011)

Figure S2.3-1 shows existing geological data and newly acquired geological data used for storage reservoir evaluation.

Table 2.3-1 List of data used for reservoir evaluation (METI,2011)

Data	purpose	data sources
3D seismic data	interpretation of geologic structure, Sedimentological study, estimation of physical property such as acoustic impedance	3D seismic data(reference: Well A, Tomakomai CCS- 1)
Core analysis data	petrological study, acquisition of basic physical properties such as porosity, permeability, relative permeability, Capillary pressure, correlation of porosity-permeability	Well A, Tomakomai CCS-1, Tomakomai CCS-2
Well velocity data	time-depth conversion of seismic data	Well A, Tomakomai CCS- 1
Wireline logging data	lithologic study including porosity/permeability, estimation of acoustic impedance	Well A, Tomakomai CCS- 1
Temperature/pressure data	thermal gradient, bottom hole pressure (reservoir pressure, fracture pressure)	Well A, Tomakomai CCS-1, Tomakomai CCS-2
2D seismic data	interpretation of geologic structure, Sedimentological study, estimation of physical property such as acoustic impedance	Existing onshore/offshore 2D seismic data

Figure S2.3-2 and Figure S2.3-3 show the results of analysis after acquisition of additional survey data. In this analysis, Well A and Tomakomai CCS-1 were used as control points of stratigraphy.

1) Takinoue Formation

The Takinoue Formation consists of the upper T1 Member of the Takinoue Formation composed of volcanic rock/tuff and the lower mudstone layer, and furthermore the T1 Member of the Takinoue Formation is divided into the upper tuff-dominated layer and the lower lava - tuff breccia-dominated layer. It was interpreted that there was a fault extending north-northeast-south-southwest along the anticlinal structure of the upper limit of the Takinoue Formation and reaching the Nina Formation. The fault throw is not uniform, and a slight throw is found near the center of the waters under study but no throw is found in the northern and southern parts. It is estimated that the reflection off the lower lava - tuff breccia-dominated layer of the T1 Member of the Takinoue Formation is generally strong, having good continuity in a horizontal direction, where coarse-grained sediments of lava - tuff breccia are distributed relatively stably.

2) Moebetsu Formation

The upper part and lower part of the Moebetsu Formation differ in the features of reflected waves. Since the reflection off the upper part is weak, having poor continuity, it is expected that siltstone - mudstone have developed; and since the reflection off the lower part is strong, having good continuity, it is expected that coarse-grained sediments (coarse-grained facies) like conglomerate and sandstone confirmed with Well A

have developed. Because this strong reflection fades and blurs as it heads southwestward, it is considered that coarse-grained facies have developed centering on the northeastern part of the waters under study. Between the sea-bottom surface and the Moebetsu Formation, reflected waves are approximately parallel, which are identified as a series of sedimentary layers. The top surface of the area developed with coarse-grained facies (the lower part of the Moebetsu Formation) is gently dipping from northwest to west.

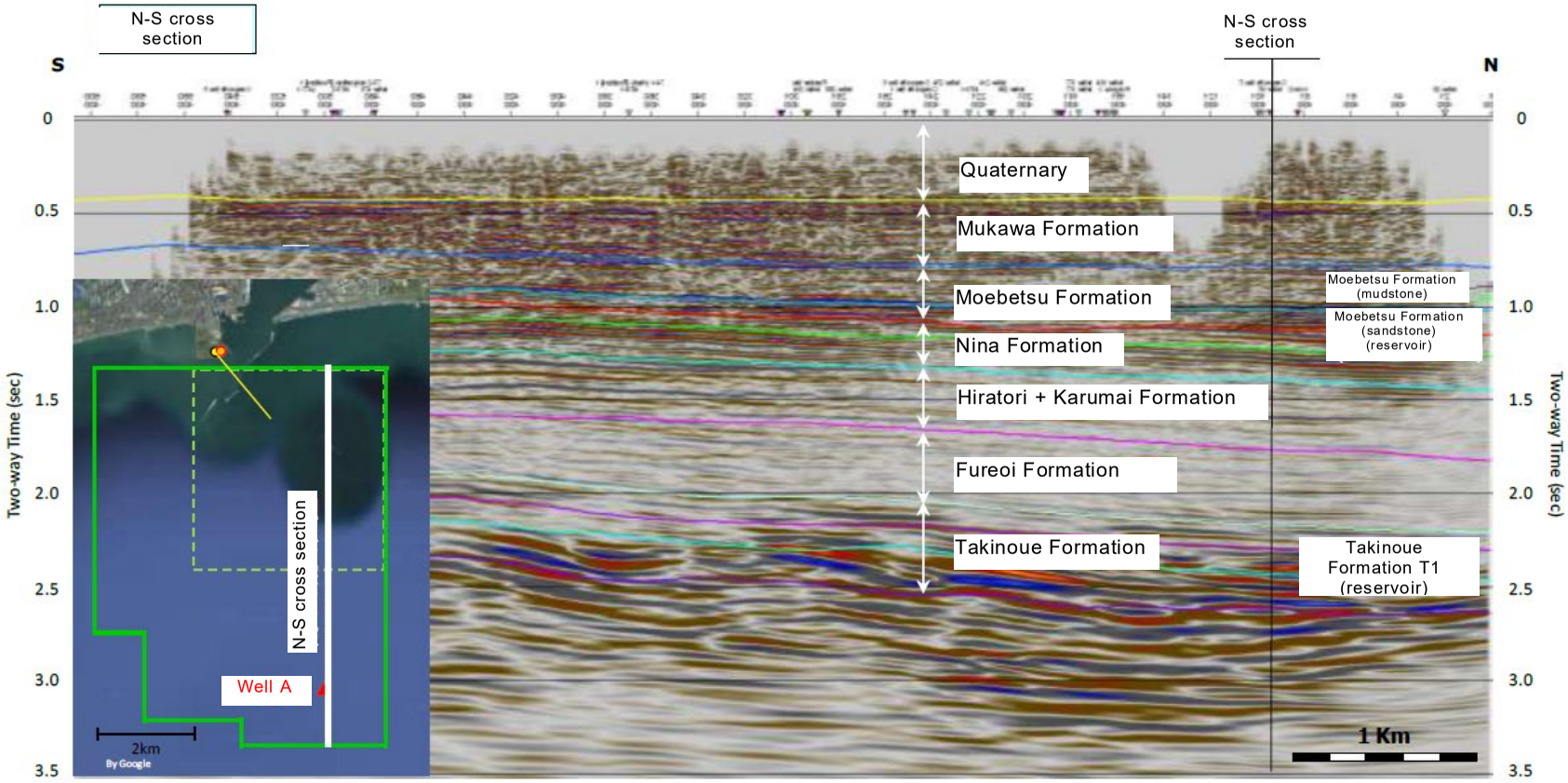

Figure S2.3-2 Cross-sectional view of the results of three-dimensional elastic wave exploration interpreted (north-south cross-section)

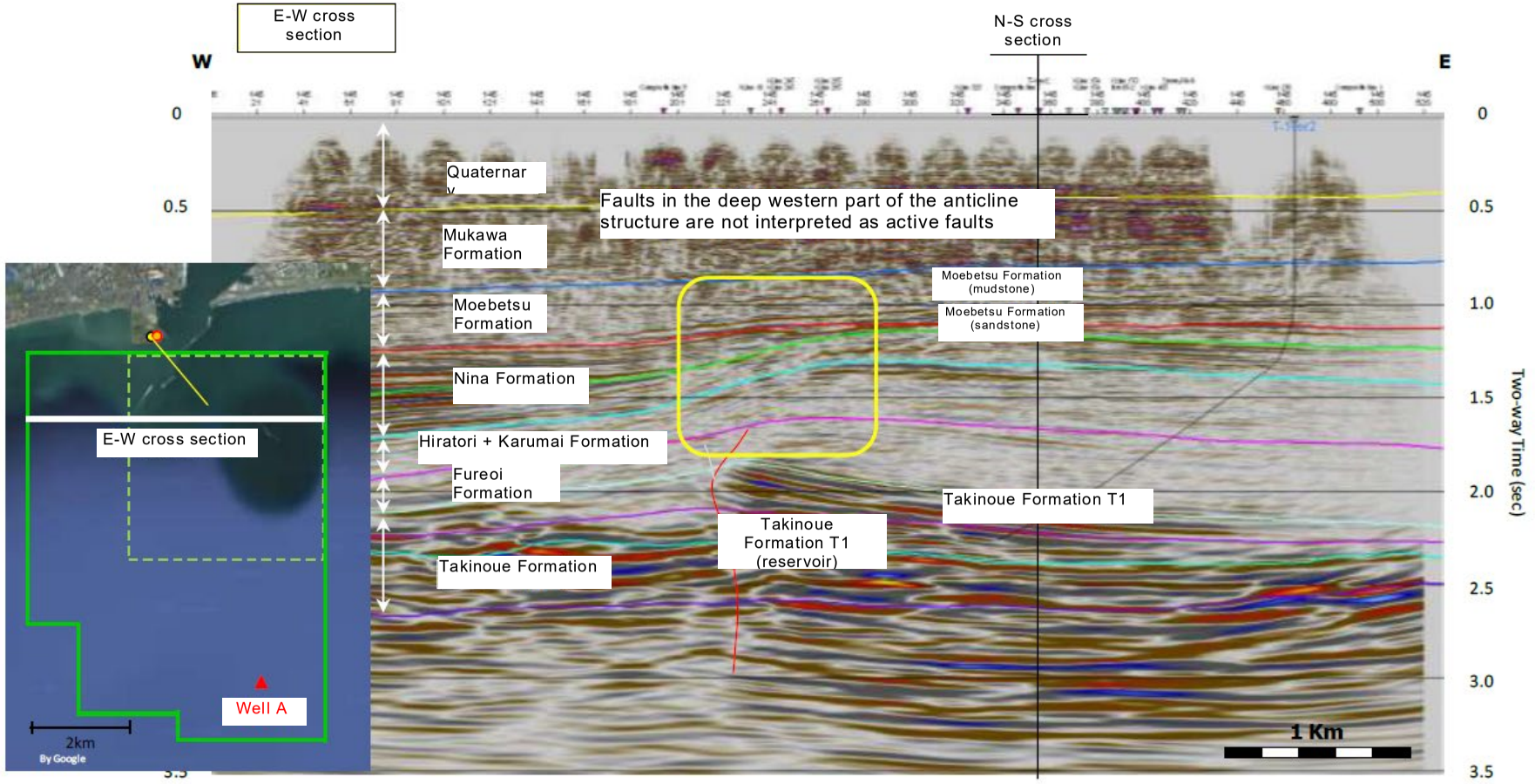

Figure S2.3-3 Cross-sectional view of the results of three-dimensional elastic wave exploration interpreted (east-west cross-section)

The geological survey results of Tomakomai CCS-1, a 3,700m deep inclined well (vertical depth: 3,046m) that was drilled in FY2010 are shown in Table S2.3-1.

Table S2.3-1 Stratigraphy and lithofacies

Formation name	drilling depth mMD (vertical depth mVD)	Lithology
Quaternary	0 -458	unconsolidated sand, pebble etc.
Mukawa F.	458-873	sand and pebble with siltstone
Moebetsu F.	873-1,230 (1211)	Mainly siltstone, mudstone(upper), sandstone(lower)
Nina F.	1,230(1211) - 1,638(1524)	Mainly siltstone-sandstone with mudstone. Unusually thin tuffaceous siltstone-sandstone, marl.
Biratori + Karumai F.	1638(1524) - 2289(2006)	Mainly siltstone-sandstone with mudstone. Unusually thin tuffaceous siltstone-sandstone, marl.
Fureoi F.	2289 (2206) - 2826(2404)	Mainly siltstone-sandstone with mudstone. Unusually thin tuffaceous siltstone-sandstone, marl.
Takinoue F. T1 Member	2826(2404) - 3700(3046)	Reworked sediments of volcanic rocks, such as volcanic breccia and tuff. Partly, pillow lava.

S2.4 Analysis results of the Takinoue Formation

S2.4.1 Storage reservoir

The Takinoue Formation is a volcanic rock layer including volcanic clastics, consisting of the T1 Member of the Takinoue Formation composed of volcanic rock/tuff and the lower mudstone layer. The T1 Member of the Takinoue Formation (approximately 600m in layer thickness) is further divided into the lower lava - tuff breccia-dominated layer and the upper tuff-dominated layer. The outline of the storage reservoir properties obtained from the site surveys is summarized in Table S2.4-1.

Table S2.4-1 List of storage reservoir properties of the T1 Member of the Takinoue Formation

ITEMS	
Depth	2,400 – 3,000m(vertical depth) approx.
Thickness	600m approx..
Lithology	lava-tuffaceous conglomerate
Porosity	5 – 18% (core test of TomakomaiCCS-1, under confining pressure) 3 -19% (core test from wells nearby, under confining pressure)
Permeability	0.68 – 1.11mD (injection test of Tomakomai CCS-1 * 0.001– 0.01mD (core test of Tomakomai CCS-1: under confining pressure, air) 0.002 – 7mD (core test from wells nearby, under confining pressure) 0.01mD – 2.6D (Interpretation of Well A wireline log)
Water injection test (Tomakomai CCS-1)	max 650Kl/day(186m interval in drilling depth 2907 -3698m)*

*From the results of pressure and temperature measurements, the injection section was determined to be 2,907 to 2,931m only.

S2.4.2 Seal layer

The Fureoi Formation and the Biratori-Karumai Formation are targeted as a seal layer, having a layer thickness of approximately 1,100m. From the results of leak-off tests at Tomakomai CCS-1, it was confirmed that the lower part of the Fureoi Formation had a strength of 1.96 in equivalent mud weight.

Despite there being a fault in the western wing of the structure at the offing of Tomakomai, it is considered that there was no vertical migration of formation water exceeding the seal layer in the past because the Fureoi Formation and the Biratori-Karumai Formation are principally composed of mudstone, and from the salt concentration distribution of formation water and the distribution of formation pressure using the peripheral well data.

With the core samples taken from the Fureoi Formation, actual measurement data of 8.2×10^{-6} to 36.7×10^{-6} mD in water permeability and 1.29MPa to 15.02 MPa or more in threshold pressure were obtained. Regarding the latter, a relatively low analysis value of 1.29 MPa was obtained, but as a result of analysis conducted under the same conditions as CO_2 storage, a value of 11.72 MPa or more was obtained.

From the above conditions and data, the Fureoi Formation and the Biratori-Karumai Formation are considered to be geological formations having good sealing performance. The outline of the seal layer properties obtained from the site surveys is summarized in Table S2.4-2.

Table S2.4-2 List of seal layer properties of the T1 Member of the Takinoue Formation

ITEMS	
Stratigraphy	Freoi F. and Biratori – Karumai F.
Lithology	mudstone
Thickness	1,100m approx.
Porosity	12.4 – 18.0% (Tomakomai CCS-1 core test: under confining pressure)
Permeability	8.2×10^{-6} – 36.7×10^{-6} mD(tomakomai CCS-1 core test, water permeability)
Threshold Pressure	> 1.29 – 12.3MPa * (Tomakomai CCS-1 core test, Aqueous residue pressure method) > 11.72MPa * (Tomakomai CCS-1 core test, Water system step boosting method) * No breakthrough was observed, so threshold pressure considered to be higher than measured value
Leak-off pressure	45.3MPa (equivalent mud eight 1.86) (leak-off test at Tomakomai CCS-1) Tomakomai CCS-1 Freoi F, 2,352m(vertical depth)

S2.4.3 Geological modeling

The Takinoue Formation, which is volcanic rock-originated, is high in non-homogeneity compared to sandstone and other sedimentary layers, and for implementation of predictive simulations of CO_2 behavior, it is especially important to estimate the spatial distribution of lithofacies and the distribution of their physical properties. Therefore, the distribution of lithofacies and the distribution of physical properties were estimated through the utilization of 3D data, which were reflected in geological structure modeling for predictive simulations of CO_2 behavior.

In order to develop storage reservoir models necessary for predictive simulations of CO_2 behavior, the time structures of respective horizons used for interpretation in 3D data were converted to depth structures.

For developing geological structure models, the horizons created by interpretation of geological structures were used: (from top, the Quaternary basement, the basement of the Mukawa Formation, the basement of the Moebetsu Formation, the basement of the upper part of the Nina Formation, the basement of the lower part of the Nina Formation, the basement of the Biratori-Karumai Formation, the upper limit of the Takinoue Formation (the basement of the Fureoi Formation), the basement of the upper part of the T1 Member of the Takinoue Formation, the basement of the T1 Member of the Takinoue Formation, and the basement of the Takinoue Formation). The positions of cross-sections of the depth-converted model of the upper limit of the T1 Member of the Takinoue Formation are shown in Figure S2.4-1, and the east-west cross-sections of major horizons (cross-sections of geological models) are shown in Figure S2.4-2.

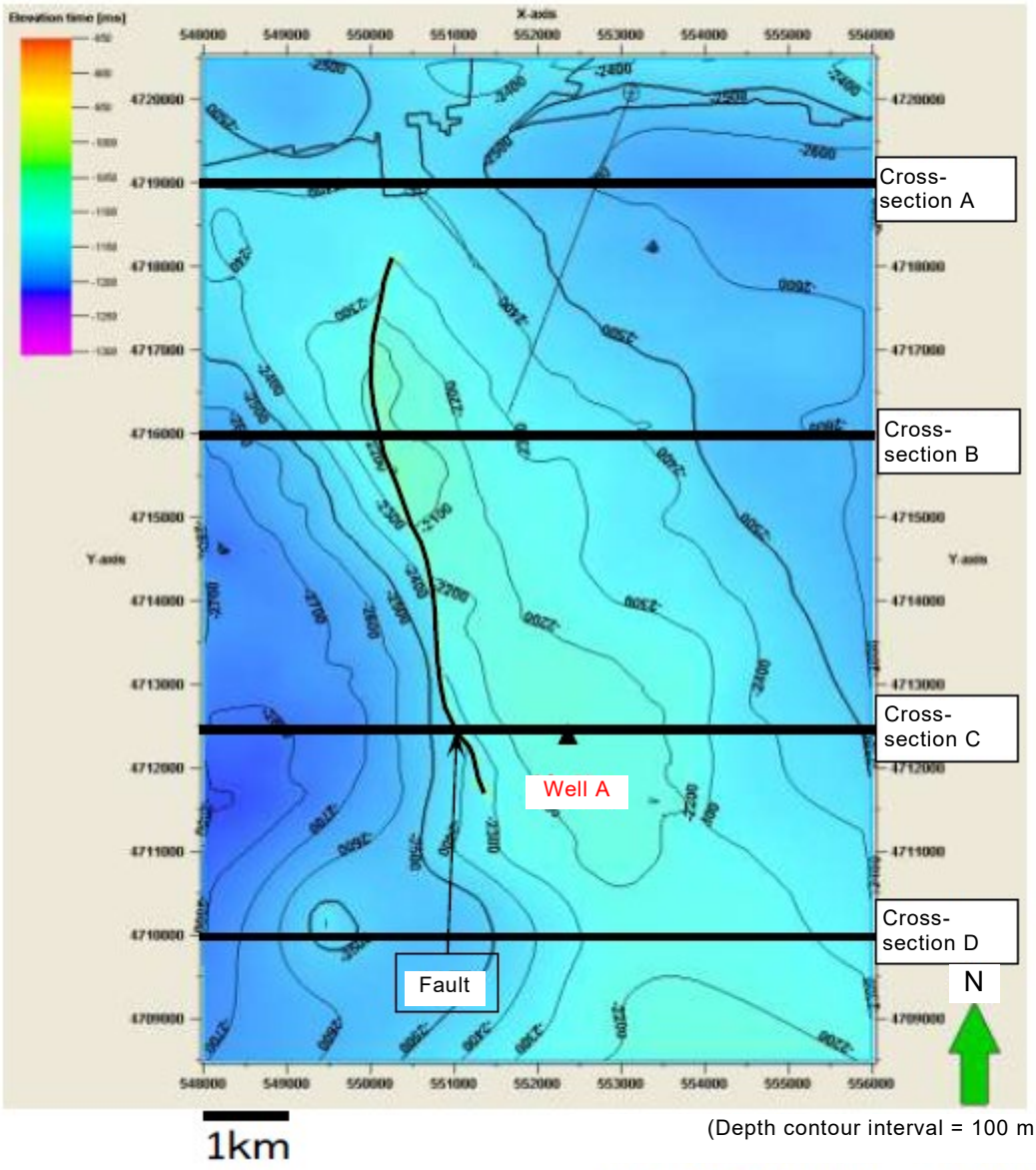

Figure S2.4-1 Model cross-section positions

(The structural drawing shows the upper limit of the T1 Member of the Takinoue Formation)

(The x-axis and y-axis in the drawing indicate coordinates on the World Geodetic System WGS84)

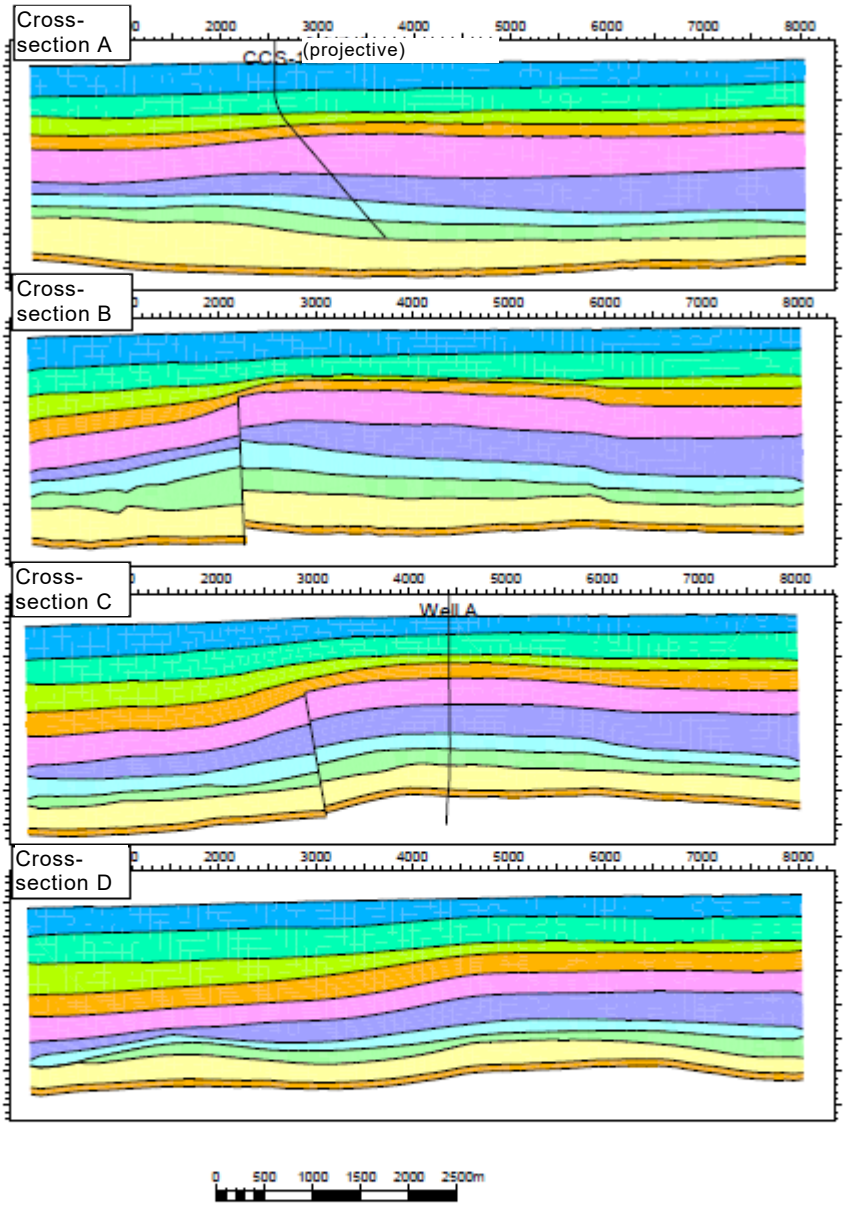

Figure S2.4-2 Geological model cross-sections

(Tomakomai CCS-1 is indicated by projection)

(3) Attribute modeling

Geological models for predictive simulations of CO_2 behavior were created by giving attributes (lithofacies, porosity, and permeability) to the T1 Member of the Takinoue Formation and other horizons in the created structure models.

First, for the distribution of attribute values of the T1 Member of the Takinoue Formation, which is targeted as a CO_2 injection layer, 50 realization models for distributions of lithofacies, porosities and permeabilities were created from 3D data and the data of Tomakomai CCS-1 and Well A by using geostatistical techniques.

For attribute values of other horizons, analysis values of the cores taken from the Fureoi Formation of Tomakomai CCS-1 were uniformly distributed. By using the 50 geological models, predictive simulations of CO_2 behavior were conducted and performance evaluations of the storage reservoir and seal layer were made. During the simulations, CO_2 was injected at a rate of 250,000 tons/year for 3 years to make predictions about injectability during the period of injection and subsequent behavior of stored CO_2, etc.

S2.5 Analysis results of the Moebetsu Formation

The Moebetsu Formation is divided into the upper part composed of siltstone - mudstone (mudstone layer of the Moebetsu Formation) and the lower part principally composed of sandstone (sandstone layer of the Moebetsu Formation). It was assumed that the sandstone layer of the Moebetsu Formation was a storage reservoir, and the mudstone layer of the Moebetsu Formation was a seal layer.

S2.5.1 Storage reservoir

The sandstone layer of the Moebetsu Formation is formed by a fan delta that has accumulated on the sea shelf while advancing offshore, and is principally composed of sandstone, accompanied by sand and gravel, as well as siltstone. Showing a gentle western dip, the layer is approximately 100m in thickness. In three-dimensional elastic wave exploration, a strong reflection having good continuity is recognized at the lower part of the Moebetsu Formation, which is suggestive of development of a sand gravel layer. Since this strong reflection is prominent in the northeastern part of the area under study and it decays southward and westward, it is interpreted that the sand gravel layer has developed centering on the northeastern part. The outline of the storage reservoir properties obtained from the site surveys is summarized in Table S2.5-1.

Table S2.5-1 List of storage reservoir properties of the sandstone layer of the Moebetsu Formation (METI,2011)

ITEM	
Depth	1,100 – 1,200m(vertical depth) approx..
Thickness	100m approx.
Lithology	sandstone (fan-delta sediments with gravel sandstone and siltstone)
Porosity	25 - 40%(core test of Tomakomai CCS-1: under confining pressure) 20 – 40% (interpretation of wireline logs)
Permeability	9 -25mD (interpreted from Tomakomai CCS-1, injection test) 1 – 1,000mD (Tomakomai CCS-1 core test: under confining pressure, air) 1 – 120mD (interpretation of wireline logs)
Water injection test (Tomakomai CCS-1)	max 1,200kl/day(57.5m interval in 1,77 – 1,217m)

S2.5.2 Seal layer

The mudstone layer of the Moebetsu Formation is composed of siltstone - mudstone, the layer thickness of which is approximately 200m. Through the analysis of depositional environment by microfossil analysis, it is estimated to have been deposited stably on a relatively shallow seabed that is several ten to hundred meters in water depth. Since it can be contrasted with peripheral wells, it is considered that the range covering the storage target area has a sufficient thickness, and from the results of core tests and leak-off tests on the lower part of the mudstone layer of the Moebetsu Formation at the exploration wells, the mudstone layer of the Moebetsu Formation is considered to have good

sealing performance. The outline of the seal layer properties obtained from the site surveys is summarized in Table S2.5-2.

Table S2.5-2 List of seal layer properties of the mudstone layer of the Moebetsu Formation (METI,2011)

ITEMS	
Stratigraphy	Moebetsu F. mudstone (upper Moebetsu F.)
Lithology	siltstone – mudstone
Thickness	200m approx.
Porosity	32.4 – 37.2% (Tomakomai CCS-2 core tests: under confining pressure)
Permeability	0.80 x 10^{-3} – 1.73 x10^{-3}mD(Tomakomai CCS-2 core tests, water permeability)
Threshold pressure	
Leak-off pressure (leak-off test at Tomakomai CCS-2)	14.6MPa(equivalent mud weight:1.50) Mudstone in Moebetu F. (Tomakomai CCS-2, 991m(vertical depth)

S2.5.3 Geological modeling

(1) Structure modeling

In order to develop geological models necessary for implementation of simulations, the time structures of respective horizons interpreted by the Tomakomai 3D data were converted to depth structures.

For developing structure models, the horizons created by interpretation of geological structures were used: (from top, the upper limit of the Mukawa Formation, the upper limit of the Moebetsu Formation, the upper limit of the Transgressive Systems Tract (TST) of the Moebetsu Formation, the upper limit of the Highstand Systems Tract (HST) of the Moebetsu Formation, the basement of the upper part of the HST delta of the Moebetsu Formation, the basement of the HST of the Moebetsu Formation, and the basement of the upper part of the Nina Formation). The positions of cross-sections of the depth-converted model of the upper limit of the sandstone layer of the Moebetsu Formation (the upper limit of the HST of the Moebetsu Formation) are shown in Figure S2.5-1, and the east-west cross-sections of major horizons of models are shown in Figure S2.5-2.

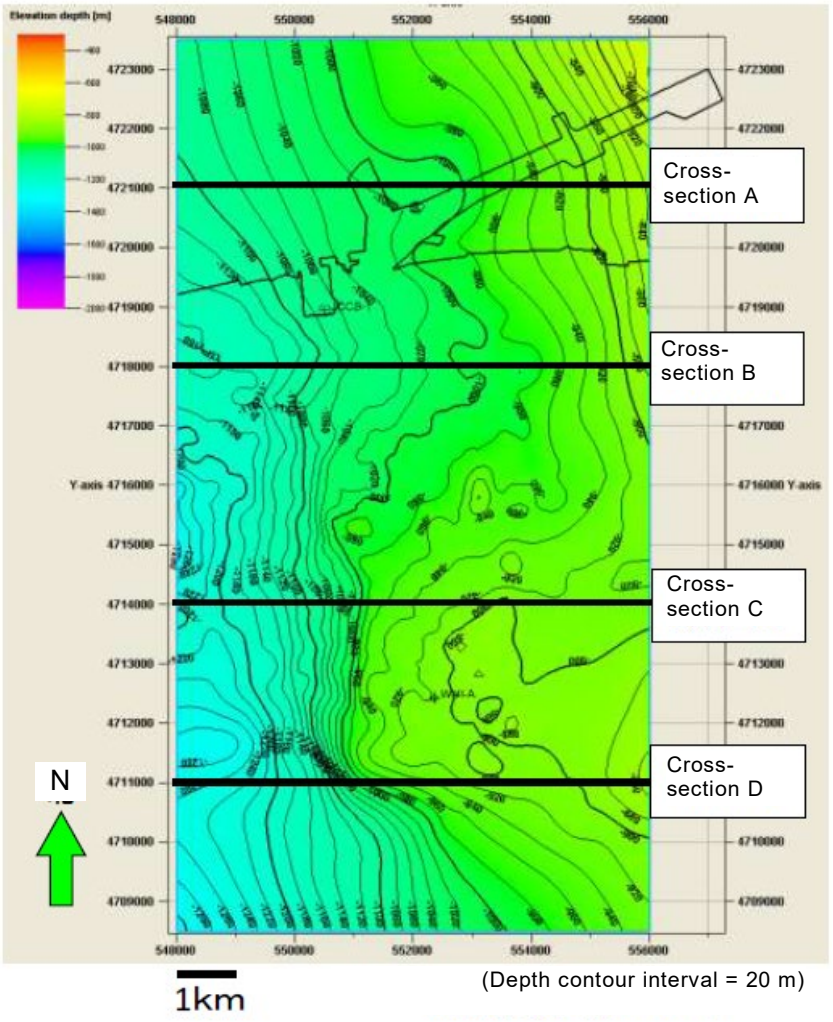

Figure S2.5-1, Location of Model cross sections on structural map of top Moebetsu sandstone highstand systems tract (METI,2011)

X,Y coordinate : World geodetic system WGS84-UTM54

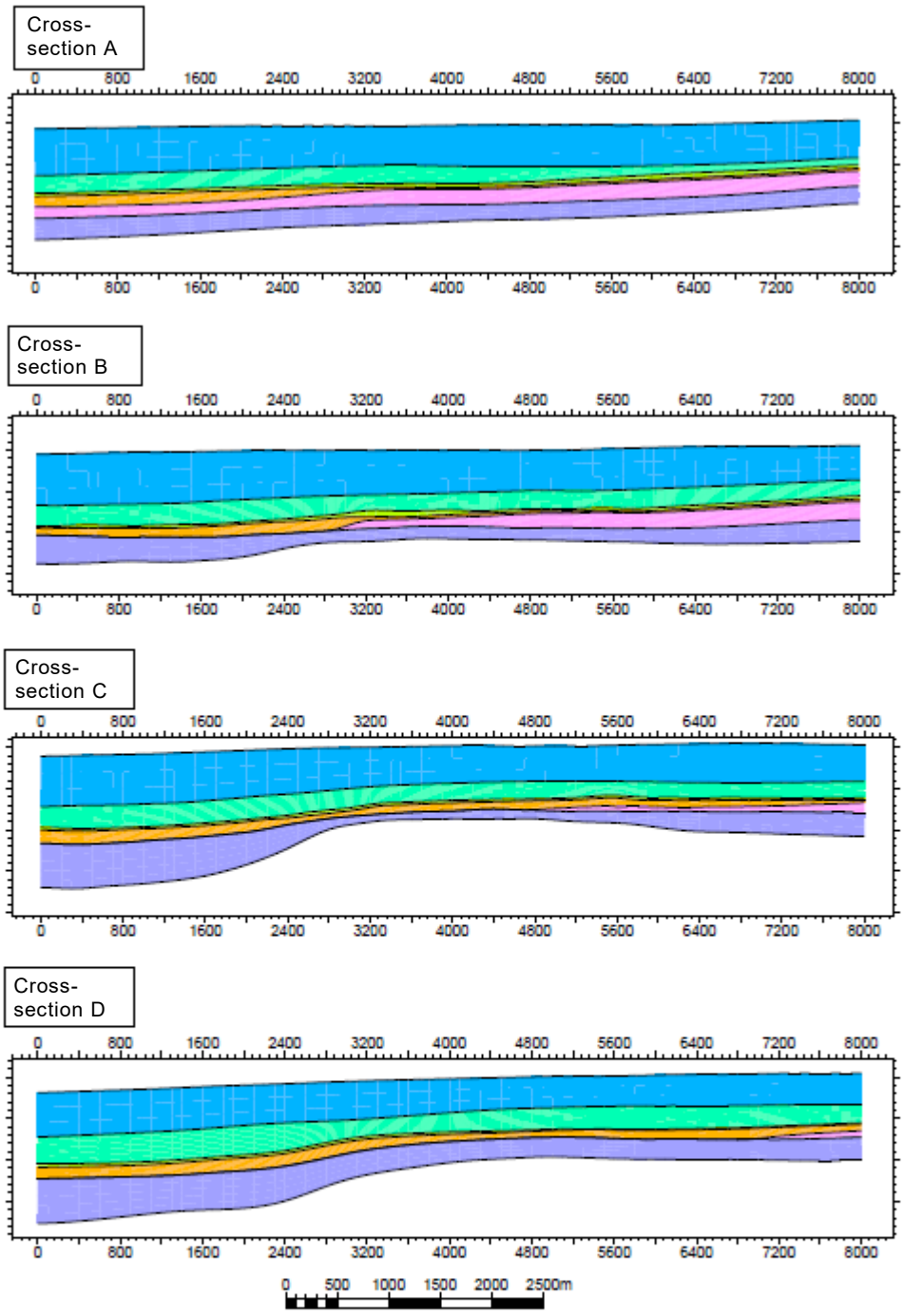

Figure S2.5-2 Model cross sections, A-D (METI,2011)

It is expected that the upper part of the Moebetsu Formation, which is a principal seal layer, has a sufficient thickness in the target area of CO_2 storage with good sealing performance. However, since a tendency of gradual thinning of the seal layer had been confirmed in the land area of the northeastern part, a thin seal layer was set in the northeastern land area.

Using storage reservoir models, predictive simulations of CO_2 behavior were conducted, and performance evaluations of the storage reservoir and seal layer were made. During the simulations, CO_2 was injected aiming for a rate of 250,000 tons/year x 3 years to make predictions about behavior of stored CO_2, etc. during the period of injection and over the following prolonged time.

S2.6 Comprehensive evaluation of the storage reservoir

In comprehensive evaluation of the storage reservoir, predictive simulations of CO_2 behavior were conducted by using the storage reservoir models developed in Chapter 2, based on the results of which the following were evaluated: whether CO_2 injection is possible as planned, whether CO_2 leakage occurs from the storage reservoir, and whether it stays in the planned range over a prolonged period of time. The evaluation results of the Takinoue Formation and the Moebetsu Formation are shown below.

S2.6.1 Evaluation results of the Takinoue Formation

(1) Storage reservoir evaluation

As described in 2.7.1, the Takinoue Formation, which is a volcanic rock layer including volcanic clastics, consists of the upper T1 Member of the Takinoue Formation composed of volcanic rock/tuff and the lower mudstone layer. The T1 Member of the Takinoue Formation (approximately 600m in layer thickness) is further divided into the upper tuff-dominated layer and the lower volcanic rock-dominated layer.

It is considered that the lava - tuff breccia facies, which are expected to be good in injection properties, can be targeted for injection as a whole; and the tuff facies, in which there are areas partly high in porosity, can be targeted for injection in part.

(2) Seal layer evaluation

As described in 2.7.2, the Fureoi Formation and the Biratori-Karumai Formation are targeted as a seal layer, having a layer thickness of approximately 1,100m. From the results of leak-off tests at Tomakomai CCS-1, it was confirmed that the leak-off pressure at the lower part of the Fureoi Formation corresponds to a strength of 1.96 in equivalent mud weight.

Despite there being a fault in the western wing of the structure at the offing of Tomakomai, it is considered that there is no vertical migration of formation water exceeding the seal layer because the Fureoi Formation and the Biratori-Karumai Formation are principally composed of mudstone, and from the salt concentration distribution of formation water and the distribution of formation pressure using the peripheral well data.

With the core samples taken from the Fureoi Formation, actual measurement data of 8.2×10^{-6} to 36.7×10^{-6}mD in water permeability and 1.29MPa to 12.3MPa or more in threshold pressure were obtained. Regarding the latter, a relatively low analysis value of 1.29MPa was obtained, but as a result of analysis conducted under CO_2-water system conditions, a value of 11.72MPa or more was obtained.

From the above conditions and data, the Fureoi Formation and the Biratori-Karumai Formation are considered to be geological formations having good sealing performance.

S2.7 Outline of simulations

① Outline

By using the developed storage reservoir models, predictive simulations of CO_2 behavior were conducted. As a simulator, Computer Modelling Group Ltd.'s GEM (ver2010.12) was used. Storage mechanisms considered during the simulations are physical trapping by capillary pressure and low permeability of mudstone, residual CO_2 trapping by residual gas saturation and gas relative permeability hysteresis, and dissolution trapping by CO_2 dissolution into formation water.

② Parameters

As simulation parameters, the values shown in Table S2.7-1 were used from the data of Tomakomai CCS-1 (injection tests, core analysis values, physical logging measurement values, etc.) and literature values.

Table S2.7-1 List of simulation parameters

Model	Takinoue F. T1 member 2011 model		
Size	8km×12km×4,000m (ideal volume 24km×24 km×4,000m)		
Grid	80×120×106 Grid		
Active block	384,050		
Reference temperature	91.0℃(2,419.4m)		
Reference pressure	34,370kPa(2,419.4m)		
injection rate, injection duration	250,000t/a×3years		
Upper limit of injection pressure	41,853kPa		
Rock character	lava(reservoir)	tuff(reservoir)	mudstone(seal)
Average porosity	0.125 Bennion(2005)	0.127	0.150
Average permeability (mD)	2.7	0.0072	0.000035
Compressibility(kPa^{-1})	8.073×10^{-7}		
Salinity (ppm NaCL)	35,100([CI^-]=21,300ppm)		
Relative permeability	lava(reservoir)	tuff(reservoir)	mudstone(seal)
Gas phase relative permeability	Bennion(2005)		Corey(1954)
Liquid phase relative permeability			van Genuchten(1980)
Critical gas saturation	0.04 Bennion(2005)		0.05
Irreducible water saturation	0.558 Bennion(2005)		0.8
Maximum Residual gas saturation	0.241 from default value of GEM		-
Capillary pressure curve	lava(reservoir)	tuff(reservoir)	mudstone(seal)
	Bennion(2006) van Genuchten(1980)		measured
Pc(kPa)	28.8	428.1	469

S2.8 Comprehensive evaluation

① Summary of the Takinoue Formation evaluations

The results of the storage reservoir and seal layer evaluations and the predictive simulations of CO_2 behavior conducted for the Takinoue Formation are summarized in Table S2.8-1 below.

Table S2.8-1 Summary of comprehensive evaluations of the storage reservoir on the T1 Member of Takinoue Formation (METI,2011)

ITEM		
Structure		- North-eastern flank of Offshore Tomakomai anticline, tending NNW-SSE - Fault cutting lower Takinoue F. to Nina F. is inferred at 2km west of injection point
Reservoir	Depth, thickness	- vertical depth 2,400 – 3,000m approx. thickenss 600m approx.
	Lithology	- lava – tuffaceous breccia, tuff
	Physical characteritics	- lava – tuffaceous breccia facies of Takinoue F. T1 member with high porosity/permeability - Porosity : 4 -18%(Tomakomai CCS-1 core test, under confining pressure) - Permeability: 0.68 – 1.18mD (Tomakomai CCS-1 injection test result) - Permeability: 0.001-0.01mD(Tomakomai CCS-1 core test: under confining pressure, air) - Permeability: 0,002 -7mD(core test of near by wells: under confining pressure) - Permeability : 0.01 – 2.6mD (interpreted from wireline logging of Well A)
	Injectivity/storage capacity	- <reservoir evaluation> lithology with high quality, inferred from 3D seismic interpretation could not recognized at appraisal well, Tomakomai CCS-1 - <simulation> 250,000 tonnes of can be injected into lithological part with high quality.
Seal	Lithology	- mudstone (Fureoi F. – Biratori F.+ Karumai F.)
	Thickness	- 1,100m approx.
	Physical character	- Porosity: 12.4 -18.0% (core test of Tomakomai CCS-1, under confining pressure) - Permeability: 8.2 x 10-6- 36.7 x 10-6mD(core test of Tomakomai CCS-1, water permeabikity) - Threshold pressure: >1.29 -12.3*MPa(Tomakomai CCS-1 core test, N2Aqueous residue pressure method) - Threshold pressure: > 11.72MPa * (Tomakomai CCS-1 core test, Water system step boosting method) *No breakthrough was observed - Leak-off pressure: 45.3MPa (equivalent mud eight 1.96) - Tomakomai CCS-1 Fureoi F, 2,352m(vertical depth)
	Seal capacity	- <simulation> did not reach to seal layer
Difficulty level of drilling well		- deep, high angle drilling
Behavior of after injection (Result of simulation)		- (3 years after injection) extent of gas phase is 400m x 600m approx. dissolved is 550m x 700m - After injection completed, down migration of by dissolution to formation water. - No more change in extent of Gas phase after 200years

(1) Comprehensive evaluation

① Summary of the Moebetsu Formation evaluations

The results of the storage reservoir and seal layer evaluations and the predictive simulations of CO_2 behavior conducted on the sandstone layer of the Moebetsu Formation are summarized in Table S2.8-2 below.

Table S2.8-2 Summary of comprehensive evaluations of the storage reservoir on the sandstone layer of the Moebetsu Formation (METI,2011)

ITEM		
Structure		- Homocline, gently dipping to the NW(1 – 3°)
Reservoir	Depth/ Thickness	- 1,100 – 1,200m(vertical depth) approx.. thickness 100m approx.
	Lithology	- sandstone (fan-delta sediments with gravel sandstone and siltstone)
	Physical characteristics	- Porosity: 25 - 40%(core test of Tomakomai CCS-1: under confining pressure), 20 - 40% (interpretation of wireline logs) - Permeability: 9 - 25mD (interpreted from Tomakomai CCS-1, injection test) - Permeability: 1 - 1,000mD (Tomakomai CCS-1 core test: under confining pressure, air) - Permeability: 1 - 120mD (interpretation of wireline logs)
	Injectivity/storage capacity	- < Tomakomai CCS-1 injection test> max 1,200kl/day(57.5m interval in 1,77 – 1,217m) - <Simulation> 250,000 tonnes /year x 3 years (except the case of low permeability)
Seal	Lithology	- iltstone – mudstone (Moebetu F.)
	Thickness	- 200m approx.
	Physical characteristics	- Porosity: 32.4 – 37.2% (Tomakomai CCS-2 core tests: under confining pressure) - Permeability: 0.80 x 10^{-3} – 1.73 x10^{-3}mD(Tomakomai CCS-2 core tests, water permeability) - Leak off pressure: 14.6MPa(equivalent mud weight:1.50 Mudstone in Moebetu F. (Tomakomai CCS-2, 991m(vertical depth) - Threshold pressure: 0.75, 1.65, 1.67Mpa(Tomakomai CCS-2 core test, Water system step boosting method)
	Seal capacity	- <simulation> At the end of injection, formation pressure at the top of reservoir(12,1MPa) does not exceed the pressure at base of seal(10.9MPa) plus threshold pressure(12.55MPa),
Difficulty level of drilling well		- Unconsolidated and soft overburden layer (Quaternary, Mukawa F.) may cause difficulty to directional and near horizontal drilling,
Behavior of after injection (Result of simulation)		- (3 years after injection) extent of gas phase is 400m x 600m, dissolved 400m x600m around injection well. - 20 years after injection, no change in extent of gas phase . - Until 1000 years later, by solution to formation water in Surrounding area, saturation is decreasing.

S2.9 Active faults distribution and seismic activity

(1) Crustal stress distribution around Hokkaido

In the "For Safe Operation of a CCS Demonstration Project," past seismic activities near the CO_2 injection point are cited as a matter to be studied for CO_2 storage from geological aspects. As part of the study of past seismic activities, there is a need to preliminarily understand the crustal stress conditions and distortion accumulation status around the injection point; therefore, the stress distribution was surveyed by using the yearly average displacement velocity vectors through the use of the GPS Earth Observation Network System (GEONET) by the Geospatial Information Authority of Japan, and the World Stress Map 2) (WSM), which is a crustal stress database.

Figure S2.9-1 shows the distribution of stress data by the WSM and displacement velocity as the Sapporo observation point is fixed. Features that are considered to reflect the stress distribution appearing in these graphics are described below.

The southeastern part of Hokkaido to the southern part of the Hidaka Mountains is an area where the collision of the Chishima arc against the Northeast Japan arc has occurred due to the subduction of the Pacific plate. The crustal displacement is prominent from east to west-northwest, which is consistent with this collision, and the displacement velocity increases as it heads southeast to reach 20mm or more annually. Although the stress data distribution chart includes only a small amount of data of land areas, there is data showing reverse fault type east-west compression near the southern edge of the Hidaka Mountains, which are harmonious with ground displacement velocity vectors.

When the Sapporo observation point existing in the Ishikari Lowland is used as a fixed point, the area from the northern part of Hokkaido to Tomakomai - Muroran is small in relative displacement.

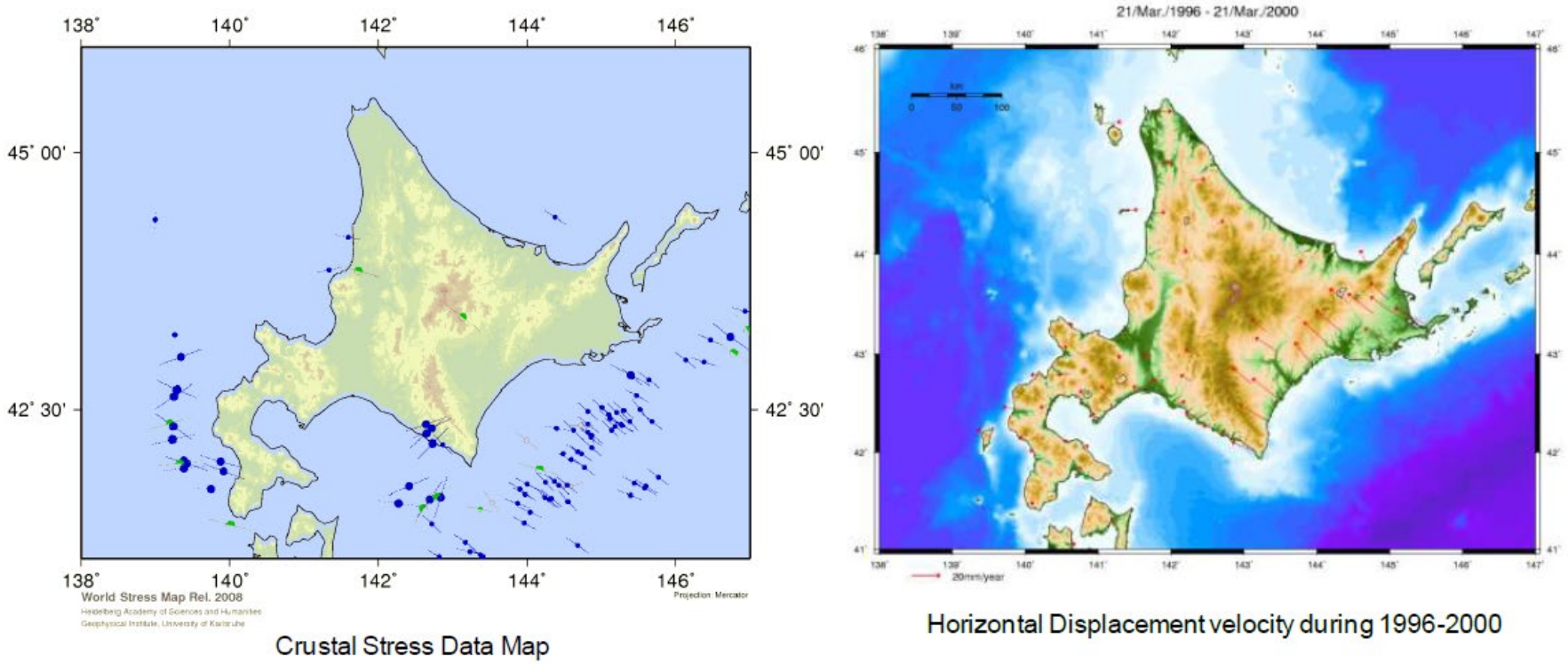

Figure S2.9-1 Crustal stress data map(left) and horizontal displacement movement velocity 1996-2000(METI,2011)

(2) Seismic activities around Hokkaido and around Tomakomai

In the "For Safe Operation of a CCS Demonstration Project," past seismic activities near the CO_2 injection point are cited as a matter to be studied for CO_2 storage from geological aspects. Therefore, surveys were conducted for the purpose of knowing the history of fault movements around the injection point and the level of crustal activities by investigating the status of past and current seismic activities.

Around Hokkaido, there are two types of seismic activities: trench type (plate boundary type) in deep portions (100km or deeper) and inland earthquakes in superficial portions (20 to 40km or shallower), and magnitude 8-class trench type massive earthquakes accompanied by tsunami have occurred repeatedly along the Chishima Trench - Japan Trench (Figure S2.9-2). It has been known from surveys on tsunami sediments that Hokkaido, having only a few old earthquakes recorded in ancient documents, has experienced massive tsunamis at intervals of every 400-500 years.

Current seismic activities around Tomakomai are shown in Figure S2.9-3. From the cross-sectional view of hypocenter distribution, it can be seen that there are 2 types of seismic activities: trench type (plate boundary type) in deep portions under the ground (100km or deeper) and inland earthquakes in superficial portions (20 to 40km or shallower). From the planar distribution chart, it can be seen that there is little difference in the level of seismic activities around the assumed point of injection from those in other areas. On the southwest side of Tomakomai City, there are active volcanos, including Mt. Tarumae, where earthquake swarms sometimes occur. In most cases, they are M5 or less, but in rare cases, they become larger than M5, causing damage locally. The active periods of such earthquake swarms are often as relatively short as 1 to 3 months, but some cases exceeding one year are also known.

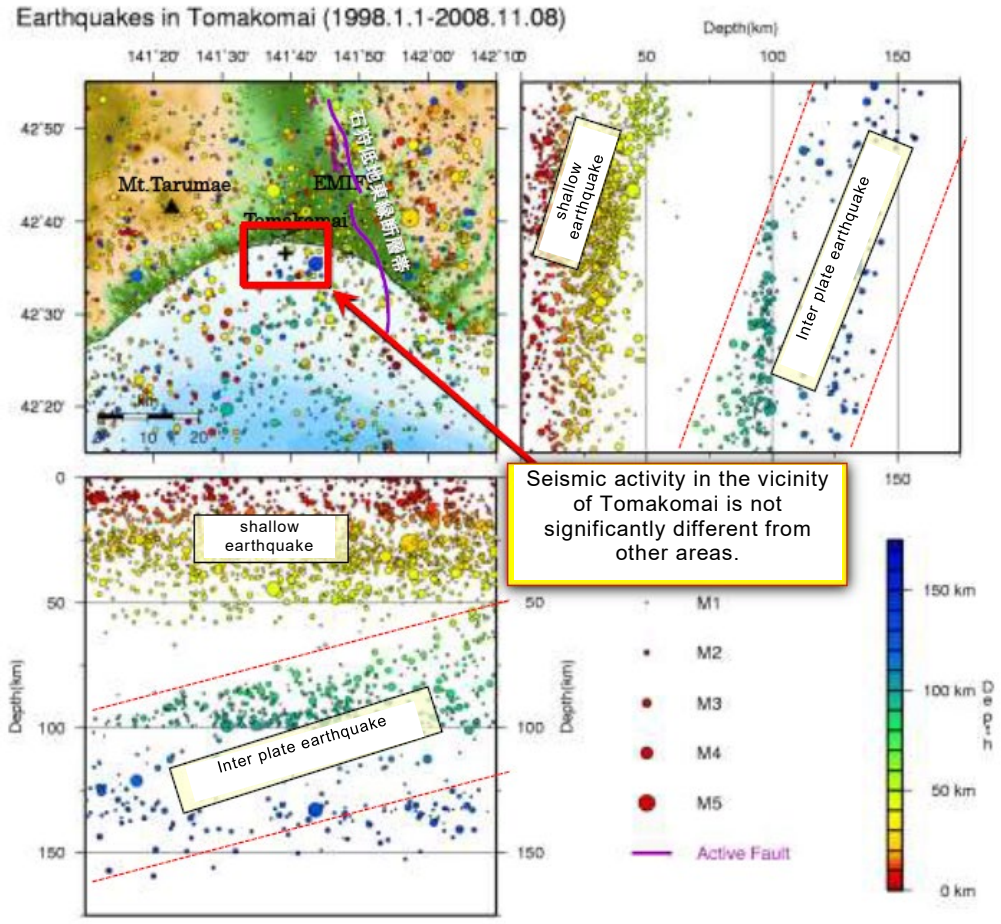

Figure S2.9-2 Earthquakes in Tomakomai 1998-2008

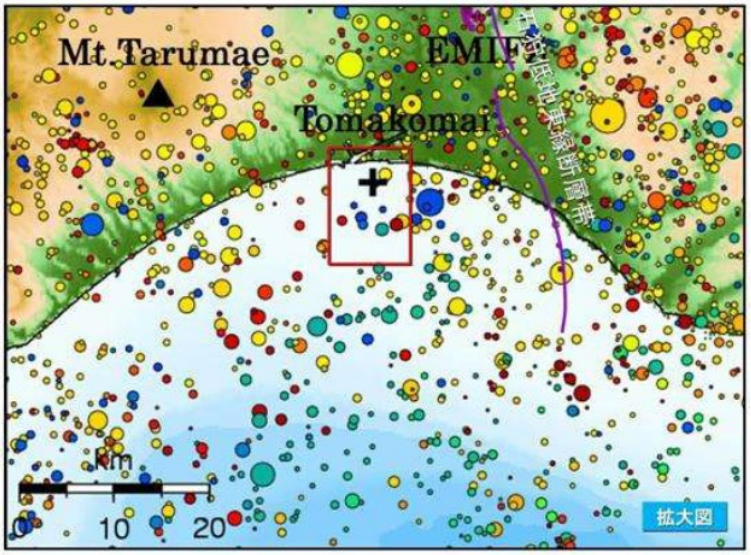

Figure S2.9-3 Recent earthquake activities around Tomakomai(1998-2008, M>1)(METI,2011)

(3) Active faults around Tomakomai

Here, active faults are defined as faults that are active from the Pleistocene Epoch within the late Quaternary

Period (approximately 130,000 years ago) until the present.

Most active faults in the Hokkaido region are reverse faults, which shows that the central part of Hokkaido is compressed roughly in the east-west direction. By crustal movement observation, it is also understood to be in a compression field approximately in the west-northwest-east-southeast direction (Figure S2.9-2).

As active faults around Tomakomai, the Eastern Boundary Fault Zone of the Ishikari Lowland lies running north-south along the eastern boundary of the Ishikari Plain (Figure S2.9-1). Figure S2.9-4 is a distribution chart of the "Eastern Boundary Fault Zone of the Ishikari Lowland" by the Headquarters for Earthquake Research Promotion. It also includes the extended portion of the southern part that was revised and added in August 2010. The extended portion of the southern part in the figure is not a fault itself but is expressed as an anticlinal structure axis representing deformations accompanied by fault activities. Faults used for predictive simulations of seismic intensity are assumed 10 to 20km east of the anticlinal axis, and are 20km or more from the assumed injection point, which can be said to be sufficiently distant.

Headquarters for Earthquake Research Promotion
"Partial revision of the evaluation of the Ishikari Lowland eastern margin fault zone (2010.08.26)"
< Extends to the southern sea area>

Item	evaluation	
Fault length	54km or more	○
Fault slope	East slope (Low angle at a depth of about 3 km or deeper, almost horizontal at a depth of about 2.5 km)	◎
Amount of one shift	About 4km or more	△
Average activity interval	Over 17,000 years	△
Assumed magnitude of earthquake	M7.7 or above	△
Earthquake probability (30 years: Poisson)	0.2% or less	d

Reliability ⇒ ◎:High, ○: Medium, △: Low
Probability of occurrence ⇒a: High, b: Medium, c: Slightly low, d: Low

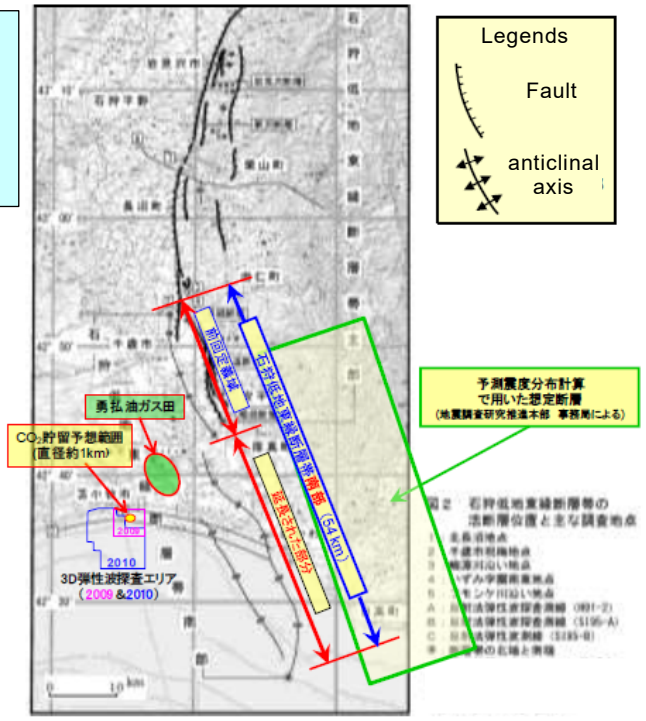

Figure S2.9-4 Eastern Boundary Fault Zone of Ishikari Lowland(METI,2011)

(4) Faults seen in cross-sectional views of three-dimensional elastic wave explorations

In the cross-sectional views of the three-dimensional elastic wave explorations that were conducted in this area, discontinuous planes judged to be faults have been confirmed. Figure S2.9-5, showing an example of this, is an east-west cross-sectional view of Line IL-145 cutting across the assumed storage point of the Takinoue Formation. The fault found nearly at the center in the cross-sectional view runs roughly in the north-south direction, cutting from the Takinoue Formation to the Biratori-Karumai Formation. This fault does not cut the Moebetsu Formation, and is estimated not to be an active fault. From the distribution shape of the Fureoi Formation through

the analysis of 3D data, this fault is estimated to be a normal fault that was formed in a pre-Middle Miocene tensile stress field. It is considered to have been followed by such activities that caused the west side to sink down at the time of sedimentation of the Nina Formation, and then the activities stopped after sedimentation of the Moebetsu Formation. Therefore, it is judged to be unlikely that the fault will become active again in the current compression stress field.

In addition, from the hydrogeological structure obtained from the salt concentration distribution of formation water, this fault is estimated to be impervious, and it is judged that the impacts of the propagation of pressure and the migration of formation water on the fault are small.

From the above, it is judged that this fault is stable against CO_2 injection into the T1 Member of the Takinoue Formation.

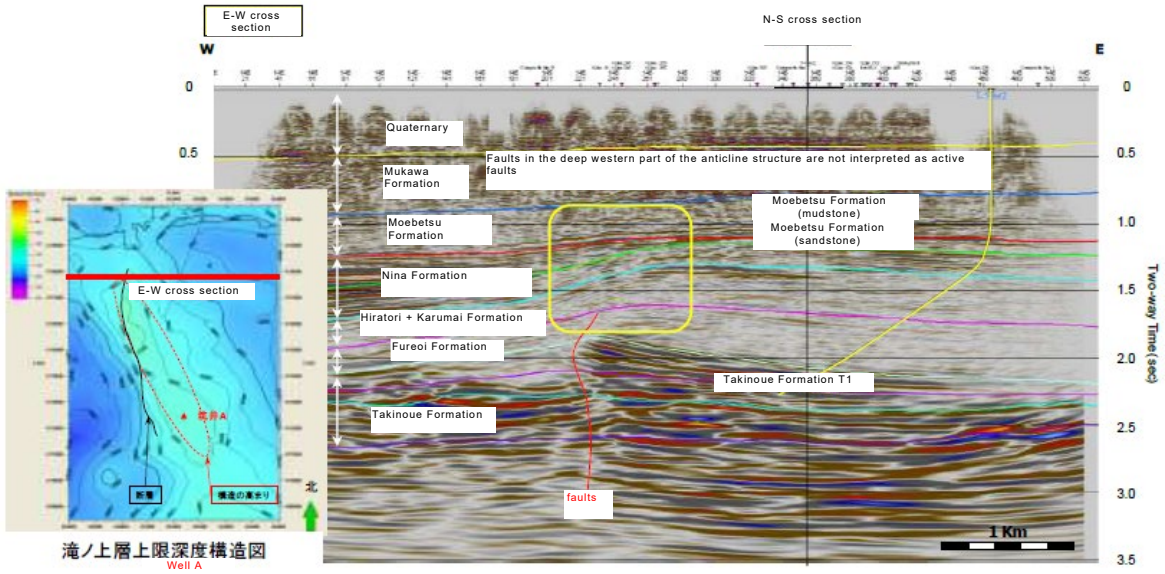

Figure S2.9-5 Example of fault on 3D seismic profile(METI,2011)

From the study results of the comprehensive evaluation of the storage reservoir at the Tomakomai site, the following leakage routes are assumed as possible factors for any leakage of stored CO_2 from the storage target layer:

1) Migration exceeding the capillarity pressure of the seal layer
2) Migration through faults
3) Migration through abandoned wells
4) Migration along the injection well and other structural objects scheduled to be installed

(5) Summary of studies related to the factors for CO_2 leakage

The results of studies on the assumed leakage routes from (1) to (4) at the Tomakomai site are summarized as follows:

1) Migration exceeding the capillarity pressure of the seal layer

The injection pressures to the T1 Member of the Takinoue Formation and the sandstone layer of

the Moebetsu Formation do not exceed the capillarity pressure (threshold pressure) of the seal layer, and CO_2 does not penetrate into the seal layer (The T1 Member of the Takinoue Formation is sufficiently high in threshold pressure. The sandstone layer of the Moebetsu Formation is lower in threshold pressure compared to the T1 Member of the Takinoue Formation, but as a result of simulation, CO_2 does not penetrate into the seal layer, where good sealing performance is expected)

2) Migration through faults

As a result of long-term predictive simulations of CO_2 behavior, there would be no change in the spread of CO_2 in about 200 years after injection, and CO_2 would not reach faults even after 1,000 years; therefore, it is considered that faults will not become a factor in CO_2 leakage.

3) Migration through abandoned wells

As a result of long-term predictive simulations of CO_2 behavior, there would be no change in the spread of CO_2 in about 200 years after injection, and CO_2 would not reach abandoned wells even after 1,000 years; therefore, it is considered that abandoned wells will not become a factor in CO_2 leakage.

4) Migration along the injection well and other structural objects scheduled to be installed

In designing and constructing the injection well and other structural objects, CO_2 migration caused by these structural objects are prevented by taking such measures as the adoption of CO_2-resistant specifications of steel materials, cement, etc. coming in contact with CO_2.

From the above, it is considered that CO_2 leakage would not occur basically through the adoption of CO_2-resistant specifications of the injection well and other structural objects.

References

1) Ministry of Economy, Trade and Industry, Industrial Technology and Environment Bureau ,Specialized study group for the implementation of CCS verification test (2011): Evaluation related to "Comprehensive evaluation of reservoir" and "Demonstration test plan (draft)" at Tomakomai site

2) Ministry of Economy, Trade and Industry, Industrial Technology and Environment Bureau , Carbon Capture and Storage (CCS) Study Group (2009):Safe implementation of CCS demonstration project

Geological Carbon Dioxide Storage
Technology Research Association

http://www.co2choryu-kumiai.or.jp/

This document is based on results obtained from a project (JPNP18006) commissioned by the New Energy and Industrial Technology Development Organization (NEDO) and Minister of Economy, Trade and Industry (METI) of Japan.